Seasonal Regulation of Petal Number[1][OPEN]

Sarah M. McKim,[a,2] Anne-Lise Routier-Kierzkowska,[b,3] Marie Monniaux,[b] Daniel Kierzkowski,[b,3] Bjorn Pieper,[b] Richard S. Smith,[b] Miltos Tsiantis,[b] and Angela Hay[b,4]

[a]Plant Sciences Department, University of Oxford, Oxford OX1 3RB, United Kingdom
[b]Max Planck Institute for Plant Breeding Research, 50829 Köln, Germany

ORCID IDs: 0000-0002-8893-9498 (S.M.M.); 0000-0003-0383-0811 (A.-L.R.-K.); 0000-0001-9220-0787 (R.S.S.); 0000-0003-4609-5490 (A.H.).

Four petals characterize the flowers of most species in the Brassicaceae family, and this phenotype is generally robust to genetic and environmental variation. A variable petal number distinguishes the flowers of *Cardamine hirsuta* from those of its close relative Arabidopsis (*Arabidopsis thaliana*), and allelic variation at many loci contribute to this trait. However, it is less clear whether *C. hirsuta* petal number varies in response to seasonal changes in environment. To address this question, we assessed whether petal number responds to a suite of environmental and endogenous cues that regulate flowering time in *C. hirsuta*. We found that petal number showed seasonal variation in *C. hirsuta*, such that spring flowering plants developed more petals than those flowering in summer. Conditions associated with spring flowering, including cool ambient temperature, short photoperiod, and vernalization, all increased petal number in *C. hirsuta*. Cool temperature caused the strongest increase in petal number and lengthened the time interval over which floral meristems matured. We performed live imaging of early flower development and showed that floral buds developed more slowly at 15°C versus 20°C. This extended phase of floral meristem formation, coupled with slower growth of sepals at 15°C, produced larger intersepal regions with more space available for petal initiation. In summary, the growth and maturation of floral buds is associated with variable petal number in *C. hirsuta* and responds to seasonal changes in ambient temperature.

The change of seasons provides predictable cues for life history transitions in plants and animals. Seasonal variation in day length and in the intensity of sunlight that warms the earth's surface provide cues for animals to hibernate or to migrate and plants to flower or seeds to be dormant. This plasticity allows organisms to maximize their performance in a complex and changing environment and is subject to genetic variation and selection. Plant flowering time is a classic example of developmental plasticity where the mechanisms of transducing environmental stimuli into plant response are well understood. While the floral transition responds to environmental cues, flower development is normally robust to environmental variation, such that a predictable number of each type of floral organ is produced in each flower. This regularity of perianth and sexual organs, in addition to being used by taxonomists for plant identification, is crucial for reproductive success by ensuring efficient pollination. But how flowers form a stereotypic and stable architecture is not well understood.

Sepals, petals, stamens, and carpels acquire their unique identities via the combinatorial action of four classes of floral organ identity genes according to the ABCE model (Coen and Meyerowitz, 1991; Pelaz et al., 2000; Honma and Goto, 2001; Krizek and Fletcher, 2005). Less is known about how a predictable number of each of these floral organs is formed; however, a key input into this process is the control of floral meristem size. For example, meristem size in Arabidopsis (*Arabidopsis thaliana*) is regulated by a negative feedback loop between WUSCHEL (WUS) and CLAVATA (CLV) proteins that maintains a stable number of stem cells in the meristem (Brand et al., 2000; Schoof et al., 2000). Loss of *WUS* or gain of *CLV3* function results in fewer floral stem cells and flowers with fewer organs (Laux et al., 1996; Brand et al., 2000). Conversely, mutations in *CLV* genes result in excess floral stem cells due to *WUS* derepression, leading to flowers with extra organs (Kayes and Clark, 1998; Fletcher et al., 1999; Schoof et al., 2000;

[OPEN] Articles can be viewed without a subscription.
www.plantphysiol.org/cgi/doi/10.1104/pp.17.00563

Clark et al., 1997). The floral stem cell pool initiates and proliferates in response to *WUS* expression during flower stages 1 and 2, prior to the activation of floral organ identity genes at stage 3, and the remaining floral stem cells differentiate in stage 6 when AGAMOUS (AG) represses *WUS* expression (Lenhard et al., 2001; Lohmann et al., 2001). Therefore, the correct number of floral stem cells is established early in floral meristem development and maintained until all four whorls of floral organs have formed.

In addition to the size of the floral stem cell pool, the timing of floral organ differentiation at stage 3 is critical to produce the correct number of floral organs per whorl. Three MADS-box genes that regulate flowering time in Arabidopsis: *SHORT VEGETATIVE PHASE* (*SVP*), *AG-LIKE24* (*AGL24*), and *SUPPRESSOR OF OVEREXPRESSION OF CO1* (*SOC1*), also regulate the timing of floral organ patterning. The proliferative phase of floral meristem maturation is cut short by precocious differentiation in *svp agl24 soc1* triple mutants, resulting in fewer floral organs (Liu et al., 2009). These flowering time regulators normally delay floral organ differentiation until stage 3 by recruiting chromatin regulators to repress expression of the class E gene *SEPALLATA3* (*SEP3*; Liu et al., 2009). In this way, SEP3 is prevented from precociously activating the floral organ identity genes *APETALA3* (*AP3*), *PISTILLATA*, and *AG* (Kaufmann et al., 2009; Liu et al., 2009). This repression is relieved once AP1 accumulates in the floral meristem and subsequently represses *SVP*, *AGL24*, and *SOC1* (Yu et al., 2004; Liu et al., 2007). *AP1* is activated by the floral regulator LEAFY (LFY; Weigel et al., 1992; Wagner et al., 1999), which also activates the expression of *AP3*, *PISTILLATA*, and *AG* (Parcy et al., 1998), such that SEP3 and LFY coordinately regulate the expression of floral organ identity genes. This regulatory loop ensures that floral organ differentiation is delayed until the floral meristem has proliferated through to stage 3. Therefore, the timing of floral meristem maturation is regulated by flowering time genes and is essential to produce a stereotypic number of floral organs per flower.

Meristem maturation in tomato plants can be modulated by genetic and environmental inputs to produce diverse shoot architectures (Park et al., 2014). For example, distinct branching patterns in both mutant and wild tomatoes can be explained by varied rates of apical and lateral meristem maturation (Park et al., 2012). This suggests that small shifts in the timing of meristem maturation can produce considerable morphological variation. However, floral meristem development is more constrained to produce a stereotypic flower with an invariant number of floral organs. For example, most plants in the Brassicaceae family have four-petal flowers, like Arabidopsis. The production of four petals in Arabidopsis requires genes that control meristem size, lateral organ outgrowth, and polarity, but also genes that confer petal identity and establish boundaries that demarcate the position of petals on the floral meristem (Irish, 2008; Huang and Irish, 2016). A critical step in this process is the suppression of growth in the regions between sepals, which creates space for auxin-induced petal initiation on the floral meristem (Huang et al., 2012; Lampugnani et al., 2013). Disrupting this mechanism, for example in double mutants between *petal loss* (*ptl*) and *auxin resistant1*, results in flowers that specifically lack petals (Lampugnani et al., 2013). Therefore, regulation of both growth and patterning in early flower development is essential to produce the stereotypic number of four petals in Arabidopsis flowers.

C. hirsuta is a close relative of Arabidopsis that shows petal number variation. Petal number in *C. hirsuta* varies from zero to four, which distinguishes its flowers from Arabidopsis and from most other Brassicaceae species. This quantitative variation characterizes *C. hirsuta* at the species level but also discriminates between different populations of *C. hirsuta*. The genetic architecture of this trait has been analyzed in five different recombinant inbred line populations of *C. hirsuta*, and at least 15 quantitative trait loci (QTL) have been identified that control petal number variation (Pieper et al., 2016). These natural alleles have small to moderate effects and influence the trait in both directions, which probably contributes to maintaining variation in *C. hirsuta* petal number (Pieper et al., 2016). Petal number also varies between individual flowers on a single plant. This variation is strongly influenced by plant ageing, such that petal number per flower declines as a plant ages. Another phenotype that shows this temporal trend is the declining number of trichomes on the abaxial side of sepals as a plant ages (Shikata et al., 2009; Yu et al., 2010), and both of these age-dependent traits share a common genetic basis in *C. hirsuta* (Pieper et al., 2016). Therefore, common QTL affect both petal number and sepal trichome number and act in an age-dependent manner. In addition, there is considerable stochastic variation in petal number between flowers initiated at the same position in isogenic individuals, which is also under genetic control (Monniaux et al., 2016). Yet significant differences in mean petal number were also observed between isogenic individuals grown in separate experiments (Pieper et al., 2016), raising the possibility that *C. hirsuta* petal number may vary in response to environmental fluctuations. Therefore, variation in *C. hirsuta* petal number is genetically determined, but it is an open question whether, and to what extent, this phenotype also responds to environmental cues.

Seasonal cues, such as day length (photoperiod), winter cold (vernalization), and ambient temperature, promote flowering of Arabidopsis in the longer, warmer days of spring in temperate regions. These cues are integrated with endogenous flowering signals, such as the age of the plant and levels of the growth hormone GA. Defined pathways transduce these external and internal signals and converge to activate flowering-promoting genes, such as *LFY* and *AP1* (Andrés and Coupland, 2012). Key genes that integrate these diverse pathways include *FLOWERING LOCUS T* (*FT*) and *SOC1* (Kardailsky et al., 1999; Kobayashi et al., 1999; Samach et al., 2000). Transport of the FT protein from where it is expressed in leaves to the shoot apex activates transcriptional reprogramming of the meristem to initiate flowering,

and *SOC1* is the earliest up-regulated gene in response to flowering cues such as day length (Samach et al., 2000; Corbesier et al., 2007; Torti et al., 2012). An age-sensing pathway that involves two microRNAs, miR156 and miR172, and their respective transcription factor targets, SQUAMOSA BINDING PROTEIN-LIKE (SPL) and APETALA2-LIKE (AP2-like) proteins, ensures that flowering does not happen until the plant is mature (Huijser and Schmid, 2011). As the plant ages, declining levels of miR156 allows *SPL* transcripts to accumulate and promote flowering, while increasing levels of miR172 relieves the floral inhibition caused by *AP2*-like genes (Mathieu et al., 2009; Wang et al., 2009; Wu et al., 2009; Hyun et al., 2016). A number of MADS-box proteins form complexes that inhibit flowering by repressing the expression of floral inducers, including *FT* and *SOC1* (Hartmann et al., 2000; Lee et al., 2007; Li et al., 2008). For example, SVP complexes with FLOWERING LOCUS C (FLC) to permit flowering only once *FLC* levels are sufficiently reduced by progressive chromatin changes in response to prolonged vernalization (Michaels and Amasino, 1999; Bastow et al., 2004; Sung and Amasino, 2004; Li et al., 2008). In addition, repressive complexes of SVP with FLOWERING LOCUS M or MADS AFFECTING FLOWERING2 decline at warmer temperatures, contributing to thermoresponsive flowering (Ratcliffe et al., 2003; Gu et al., 2013; Lee et al., 2013; Posé et al., 2013; Airoldi et al., 2015; Sureshkumar et al., 2016).

Although ambient temperature is an important signal for growth and development, the mechanisms by which plants perceive this signal are not yet fully understood. Thermosensing is an important function of the red-light photoreceptor phytochrome B in Arabidopsis, particularly at night (Jung et al., 2016; Legris et al., 2016). Phytochromes sense light by switching between an inactive and active form. Warm temperatures deplete the active phytochrome pool and disrupt the transcriptional output of phytochrome B signaling (Jung et al., 2016; Legris et al., 2016). In this way, temperature information is perceived and transduced through the light-sensing pathway to regulate thermomorphogenesis. The histone variant H2A.Z is another potential thermosensor (Talbert and Henikoff, 2014). It has been proposed that nucleosomes containing H2A.Z wrap DNA more tightly than H2A-containing nucleosomes, making it less accessible for transcription factors (Kumar and Wigge, 2010). H2A.Z nucleosomes are depleted at warmer temperatures, providing a mechanism for temperature-regulated expression of genes such as *FT* (Kumar and Wigge, 2010). Therefore, these mechanisms are likely to contribute to the thermoresponsiveness of growth and flowering in Arabidopsis.

Here, we find seasonal variation in the number of petals produced by *C. hirsuta* flowers. Spring flowering plants produce more petals per flower than summer flowering plants. We characterize the developmental plasticity of petal number and show that it varies in response to a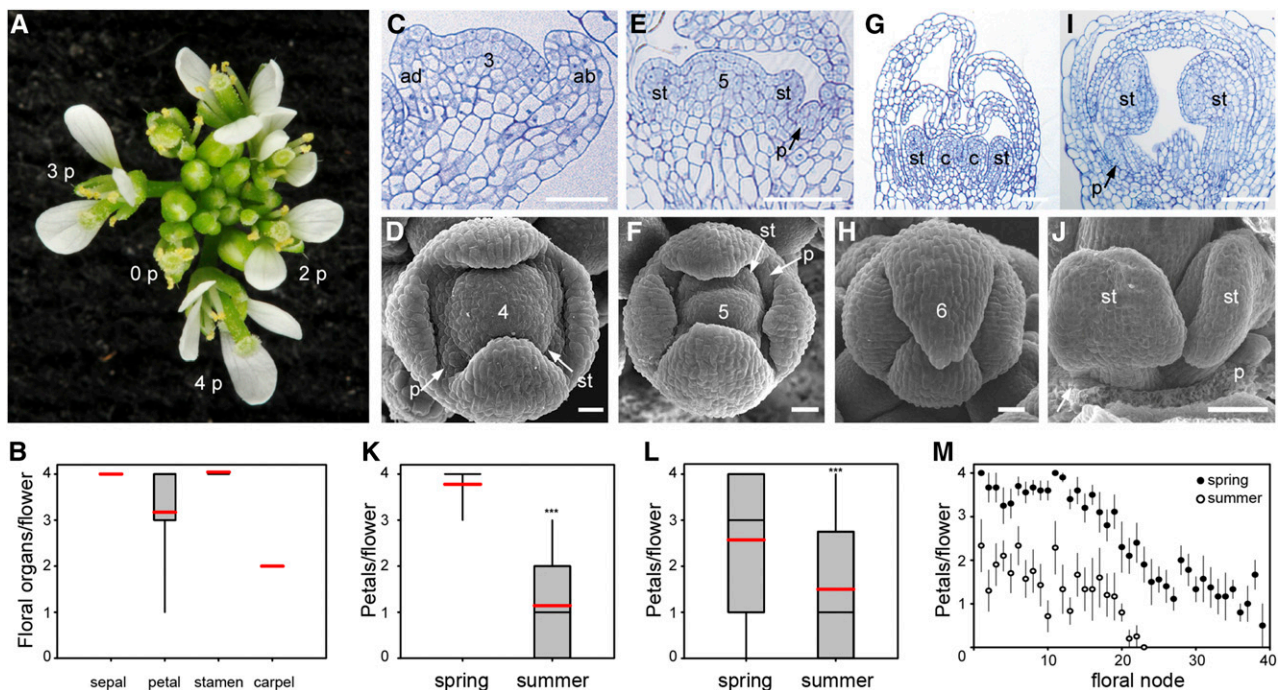mbient temperature, photoperiod, simulated shade, vernalization, and GA levels. In particular, we show that cooler temperatures, experienced by plants flowering in spring compared to summer, strongly correlate with a higher number of petals per flower. Using live imaging to quantify growth at early stages of flower development, we show that the maturation of floral buds is more gradual at cooler temperatures, resulting in wider regions between sepals that influence petal initiation.

RESULTS

Petal Number Varies According to Season and Age

Petal number varies from zero to four among the flowers produced by an individual *C. hirsuta* plant (Fig. 1A). Variation in floral organ number is mostly restricted to petals, as *C. hirsuta* flowers produce a fixed number of four sepals and two carpels (Fig. 1B). *C. hirsuta* flowers usually lack the two lateral stamens present in Arabidopsis (Fig. 1B), although lateral stamen number can vary in both species (Muller, 1961; Smyth et al., 1990; Hay et al., 2014). Variation in the number of lateral stamens and petals is not correlated in *C. hirsuta* (Supplemental Table S1; $r = 0.11$). To investigate the developmental basis of petal number variation, we examined the ontogeny of floral organs in *C. hirsuta* (Fig. 1, C–J; Supplemental Fig. S1; Supplemental Tables S1 and S2). Sepals initiated first, forming creased buttresses in stage 3 meristems, growing over the floral meristem at stage 5 to completely enclose the floral bud by stage 6 (Fig. 1, C–H). Petal primordia developed just interior to the intersepal regions at stage 4, and two pairs of medial stamen primordia emerged interior to petals on the floral meristem (Fig. 1D). By stage 5, small petal and stamen primordia were clearly visible (Fig. 1, E and F). Carpel primordia consumed the center of the floral meristem in stage 6 flowers where the sepals had enclosed the bud and interleaved at their tips (Fig. 1, G and H). Small petal primordia were either clearly present or absent at the base of well-developed stamens in stage 8 flowers when viewed in longitudinal sections or scanning electron micrographs with obscuring sepals dissected away (Fig. 1, E, G, I, and J). Therefore, the variable petal number observed in mature *C. hirsuta* flowers seems to originate from early events during petal initiation, rather than later events in petal growth.

To investigate the relevance of petal number variation for the natural growth of *C. hirsuta*, we counted petal number in local stands of *C. hirsuta* around Oxford, UK. We found that petal number varied in all the plants we counted, similar to our observations in greenhouse conditions (Fig. 1K). But what was striking was the seasonal difference in average petal number between spring- and summer-flowering *C. hirsuta* plants. Local stands of *C. hirsuta* that flowered in summer months (July/August) produced an average of only 1.14 ± 0.08 petals per flower compared to 3.78 ± 0.03 petals per flower in populations that flowered in

Figure 1. Petal number varies according to season and age in *C. hirsuta*. A, Petal number varies between zero (0 p) and four (4 p) in the flowers of a single inflorescence in *C. hirsuta*. B, Box plot of floral organ counts per flower in *C. hirsuta*. C, Longitudinal section through a stage 3 floral bud shows growth of the abaxial (ab) sepal is advanced compared to the adaxial (ad) sepal. D, Scanning electron micrograph of a stage 4 floral bud shows outgrowth of all four sepals and early petal and stamen primordia. E and F, Longitudinal section (E) and scanning electron micrograph (F) of stage 5 floral buds show sepals growing over the floral meristem, prominent stamen primordia, and small petal primordia. G and H, Longitudinal section (G) and scanning electron micrograph (H) of stage 6 flowers show sepals enclosing the bud with their tips folding within the bud. Section shows developing stamen and carpel primordia but no petal primordia. I and J, Longitudinal section (I) and scanning electron micrograph (J) of older floral buds show that petal primordia are either present or absent (arrow, J) in whorl two. K, Box plot of petals per flower in spring and summer flowering populations of *C. hirsuta*, $n = 419$ flowers. L, Box plot of petals per flower in the *C. hirsuta* Ox accession grown in late spring and summer field conditions, $n = 468$ flowers. M, Average petal number per flower at consecutive floral nodes in *C. hirsuta* Ox plants grown in summer (white circles) and late spring (black circles) field conditions, $n = 10$ plants in each condition, error bars show SE. The first floral node is labeled as 1. Pairwise comparisons by Mann-Whitney *U* test. Significance levels: ***$P < 0.001$, **$P < 0.01$, *$P < 0.05$. Box plots show 25th to 75th percentiles; whiskers extend down to 10th and up to 90th percentiles; black line shows median; red line shows mean. Numbers in C to H indicate floral stage; st, stamen; p, petal; c, carpel. Scale bars = 20 μm (C–J).

spring months (March/April; Fig. 1K). This difference was highly significant ($P < 0.001$, Mann-Whitney *U* test). To understand what component of this seasonal trend might reflect developmental plasticity versus genetic differences between populations, we grew isogenic *C. hirsuta* plants under field conditions in different seasons. We performed these experiments at a field site at MPIPZ, Cologne, Germany, during April/May 2016 (spring) and August 2016 (summer), using the *C. hirsuta* Ox accession. We found a highly significant difference in petal number between these flowering seasons: Summer-flowering plants produced on average only 1.48 ± 0.11 petals per flower compared to 2.65 ± 0.08 petals per flower in spring-flowering plants (Fig. 1L; $P < 0.001$, Mann-Whitney *U* test). Therefore, the flowers of isogenic *C. hirsuta* plants vary their petal number in response to seasonal cues.

To investigate the environmental regulation of *C. hirsuta* petal number, we examined climate data recorded at the Cologne field site during our experiments. Although numerous climatic conditions, including day length, differed between these spring and summer field experiments (Supplemental Fig. S2), we found a large difference in mean daily temperature (spring, 13.5°C ± 0.6°C; summer, 19.3°C ± 0.5°C; $P < 0.001$, Mann-Whitney *U* test; Supplemental Fig. S2). Thus, *C. hirsuta* plants flowering in spring experienced lower ambient temperatures and produced higher petal numbers than summer-flowering plants.

In addition to this seasonal trend, we had previously described a temporal trend in petal number during plant ageing in *C. hirsuta* (Monniaux et al., 2016; Pieper et al., 2016). We found that average petal number per flower also declined as the plants aged in field conditions (denoted by floral node number, Fig. 1M), similar

to greenhouse-grown plants (Monniaux et al., 2016; Pieper et al., 2016). This trend was apparent in the *C. hirsuta* Ox accession, irrespective of whether the plants flowered in spring or summer (Fig. 1M). However, the lower average petal number in summer-flowering plants was reflected in lower petal numbers at all floral nodes (Fig. 1M). In addition, fewer flowers were produced in summer- compared to spring-flowering plants (Fig. 1M). Therefore, both endogenous ageing and external environmental cues regulate petal number variation in *C. hirsuta.*

C. hirsuta Flowers in Long Days

Since flowering time in Arabidopsis also responds to ageing and seasonal cues, we first characterized this process in *C. hirsuta*, before further exploring how these same cues might affect petal number. To describe how photoperiod influences the floral transition in *C. hirsuta*, we grew plants for 3 weeks in moderately short days (10 h light:14 h dark), where the plants produced a vegetative rosette (Fig. 2A) and then transferred the plants to long days (16 h light:8 h dark). Within 5 to 6 d after transfer, the apical meristem switched from producing leaf primordia to floral buds (Fig. 2, B–D). The inflorescence later bolted to produce an indeterminate raceme bearing secondary flowering branches and single lateral flowers (Fig. 2E). For the first 11 d after transfer to long days, almost three floral buds were produced per day before slowing to a rate of one to two buds per day (Fig. 2F). To examine the photoperiodic induction of flowering at a molecular level, we measured transcript levels of the *C. hirsuta AP1* and *SVP* genes (*ChAP1* and *ChSVP*) in vegetative seedlings, early inflorescence meristems (~5 to 10 floral buds produced) and in inflorescences at anthesis (Fig. 2G). Levels of *ChAP1* mRNA doubled in early inflorescence meristems, while inflorescence shoots at anthesis showed a 21-fold increase, likely due to the high number of developing flowers at this stage (Fig. 2G). *ChSVP* expression levels increased from the vegetative to early inflorescence to older inflorescences at anthesis, probably due to the increasing number of early floral buds (Fig. 2G). Taken together, these data show that long-day photoperiods induce flowering in *C. hirsuta.*

To determine the relationship between photoperiod length and floral induction, we compared flowering time in *C. hirsuta* plants grown under short-day (8 h:16 h light/dark), neutral-day (12 h:12 h light/dark), and long-day (16 h:8 h light/dark) conditions. We assessed the floral transition morphologically, by counting the total number of rosette leaves produced, and temporally, by recording the number of days postgermination when floral buds became visible on the inflorescence, when the bolting stem reached 5 cm, and at anthesis. We found that these temporal measures of flowering time were largely correlated (Supplemental Fig. S3), so we report the timing of visible floral buds throughout. We defined the floral maturation interval as the number of days between the appearance of floral buds and anthesis. Consistent with our previous experiment, we found that flowering time in *C. hirsuta* was significantly accelerated by growth in long days, as plants produced fewer rosette leaves and transitioned earlier to flowering (Fig. 2H). Compared to neutral days, floral maturation was particularly fast in long-day conditions but also accelerated in short days (Fig. 2H). Growth in short days significantly delayed the time to flowering, compared to other photoperiods, although plants produced a similar number of rosette leaves in both neutral and short days (Fig. 2H; Supplemental Fig. S3). Altogether, our data suggests that the critical photoperiod for floral induction in *C. hirsuta* lies between 8 and 12 h.
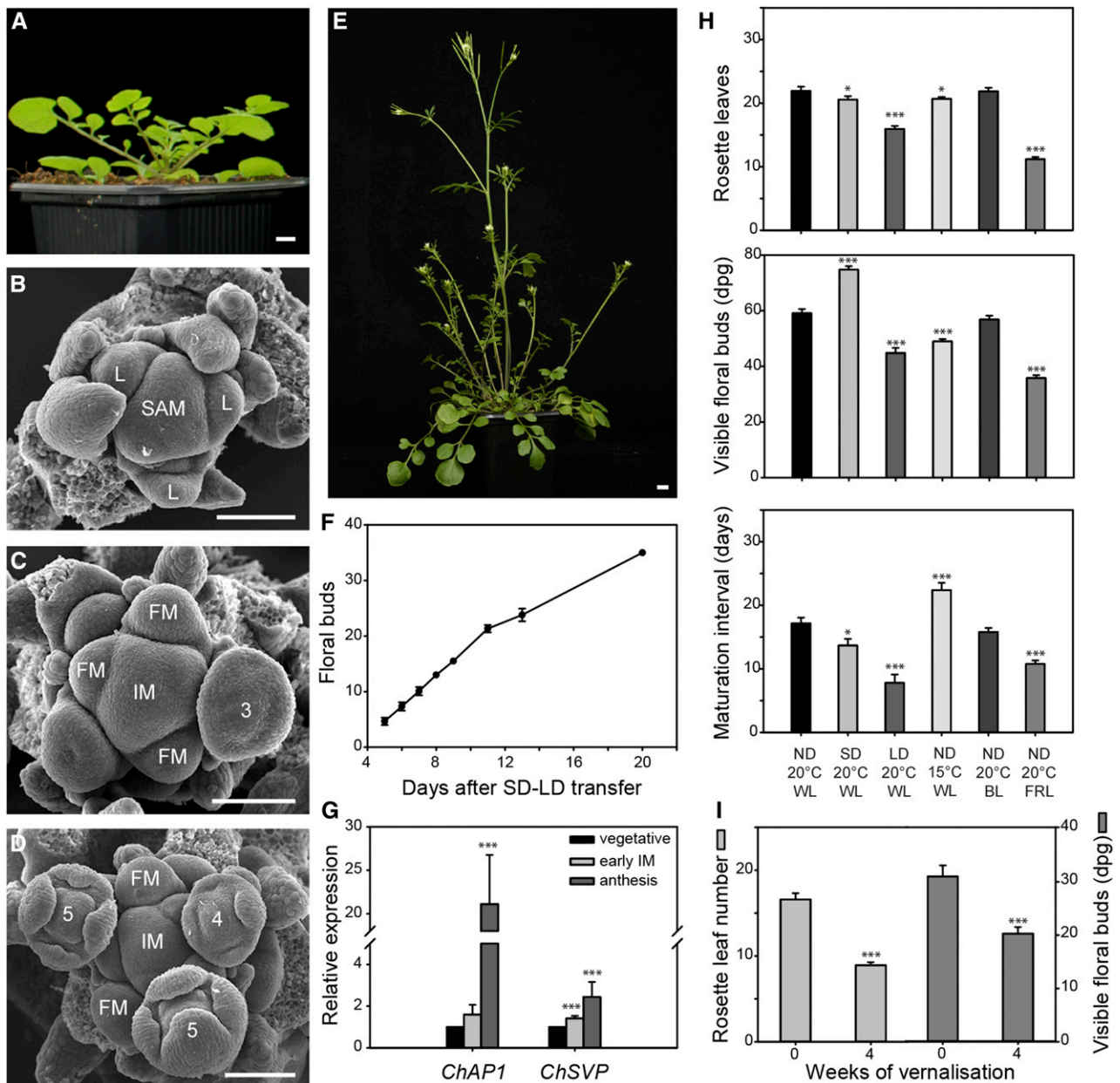
Onset of Flowering in *C. hirsuta* Is Accelerated by Simulated Shade, Cooler Ambient Temperatures, and Vernalization

To investigate the effect of other external cues on *C. hirsuta* flowering time, we altered light quality and temperature under neutral day conditions in order to minimize the effects of photoperiod (Fig. 2, H and I; Supplemental Tables S3 and S4). Growth in far-red light significantly accelerated flowering time in *C. hirsuta* (Fig. 2H). This is a typical shade avoidance response to simulated shade conditions. These plants produced fewer rosette leaves, transitioned earlier to flowering, and showed rapid maturation of floral buds to flowers (Fig. 2H). Growth in blue light on the other hand, did not affect flowering time (Fig. 2H).

We found that flowering time was significantly accelerated at cooler ambient temperatures when plants were grown at 15°C compared to 20°C (Fig. 2H). However, growth at 15°C also resulted in very slow floral maturation (Fig. 2H). Therefore, at cooler temperatures, floral buds matured into flowers over a much longer time interval, despite an accelerated flowering time. We also determined that flowering time in *C. hirsuta* responded to vernalization. Growth at approximately 4°C for up to 4 weeks significantly accelerated the transition to flowering and resulted in fewer rosette leaves (Fig. 2I; Supplemental Fig. S3). Given that *C. hirsuta* plants responded to vernalization and that plants in our neutral day conditions experienced cool (15°C) temperatures for approximately 50 d of vegetative growth, the accelerated flowering we observed at 15°C may reflect a mild vernalization response. Taken together, our findings suggest that both flowering time and floral maturation in *C. hirsuta* are sensitive to environmental control.

Petal Number Is Sensitive to Environmental Cues

To further investigate the relationship between petal number variation and environment that we observed in our spring versus summer field experiments, we determined whether petal number responded to the same

Figure 2. *C. hirsuta* flowering is accelerated by long days, vernalization, cool ambient temperature, and simulated shade. A, *C. hirsuta* vegetative rosette. B to D, Scanning electron micrographs of *C. hirsuta* plants following SD to LD transfer. B, shoot apical meristem (SAM) initiating leaf primordia (L) 4 d after transfer; C, inflorescence meristem (IM) initiating floral meristem primordia (FM) 5 d after transfer with the oldest primordium at stage 3; D, IM initiating FM 6 d after transfer with the oldest primordium at stage 5. E, *C. hirsuta* flowering raceme. F, Line graph shows cumulative floral bud production starting 5 d after SD to LD transfer. G, Relative expression levels of *ChAP1* and *ChSVP* mRNA in vegetative SAM, early IM (5–10 floral buds), and IM at anthesis, shown as fold change of vegetative levels. Expression is compared pairwise to vegetative samples. H, Flowering time, measured as number of rosette leaves and number of days after germination when the first floral buds are visible, and floral maturation interval, measured as the number of days between visible floral buds and anthesis, were compared between different photoperiods, ambient temperatures, and light qualities. ND, Neutral days (12:12); SD, short days (8:16); LD, long days (16:8); WL, white light; BL, blue light; FRL, far-red light. I, Flowering time, measured as number of rosette leaves (left *y* axis) and visible floral buds (right *y* axis), in response to vernalization at ~4°C. Pairwise comparisons by Mann-Whitney *U* test. Significance levels: ***$P < 0.001$, **$P < 0.01$, *$P < 0.05$. $n = 26$–28 (ND, 20°C, WL); $n = 7$–26 (LD, 20°C, WL); $n = 26$–29 (SD, 20°C, WL); $n = 12$–31 (ND, 15°C, WL); $n = 29$–31 (ND, 20°C, FRL); $n = 22$–31 (ND, 20°C, BL); $n = 12$ (vernalization). Error bars show SE. Scale bars = 1 cm (A and E) and 100 μm (B–D).

environmental cues that affected flowering time in *C. hirsuta*. Specifically, we recorded petal number in the same experiments described above where we measured flowering time (Supplemental Tables S3 and S4). Plants grown in short days produced, on average, twice as many petals per flower (1.53 ± 0.06) compared to plants grown in long days (0.69 ± 0.06) or neutral days (0.68 ± 0.07; Fig. 3A). Therefore, the difference between a 12-h and 16-h photoperiod significantly affected petal number ($P < 0.05$, Tukey Kramer). Simulated shade (far-red light) also increased petal number compared to white or blue light ($P < 0.01$, Tukey Kramer; Fig. 3A, Supplemental Fig. S4) as did 4 weeks of vernalization at approximately 4°C ($P < 0.05$, Tukey Kramer; Fig. 3B, Supplemental Fig. S4). But we found that cool ambient temperature produced the most significant increase in petal number: Plants grown at 15°C developed an additional ~2.5 petals per flower compared to those at 20°C, a greater than 4.5-fold increase ($P < 0.001$; Fig. 3A). This variation in petal number in response to ambient temperature showed a positive correlation with the interval of floral maturation ($r = 0.63$, Pearson coefficient of correlation, $P < 0.05$). Therefore, petal number increases when the maturation of floral buds is more gradual at cooler temperatures.
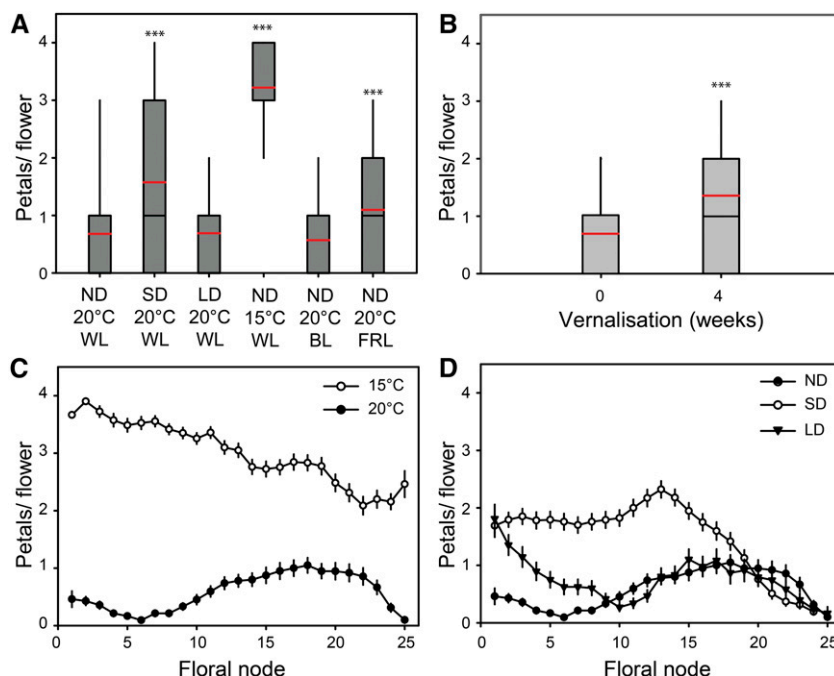
To understand how distinct environmental factors influenced petal number during the progressive ageing of the plant, we assessed petal number at each successive floral node. A cooler ambient temperature of 15°C dramatically increased the number of petals per flower at all floral nodes, reflecting a sustained influence throughout the ageing of the inflorescence (Fig. 3C). This pattern of higher overall petal number, within the context of a decline in petal number during ageing, is similar to what we observed in spring versus summer flowering plants in the field (Fig. 1M). Moreover, the difference in mean daily temperature recorded at the field site (spring, 13.5°C $\pm$ 0.6°C; summer, 19.3°C $\pm$ 0.5°C), was similar to the temperature difference used in our controlled environment experiments (15°C versus 20°C), suggesting that ambient temperature was likely to be a major factor influencing petal number in the field experiments. Growth in short-day conditions increased the number of petals per flower for the first 17 floral nodes before declining at later floral nodes to the same values as long-day- or neutral-day-grown plants (Fig. 3D). Therefore, the small difference in average day length between spring (15.3 h $\pm$ 0.1) and summer (14.3 h $\pm$ 0.1) field experiments is unlikely to be sufficient to explain the observed difference in petal number (Fig. 1M). In summary, different environmental factors have distinct effects on the age-dependent decline in petal number in *C. hirsuta*.
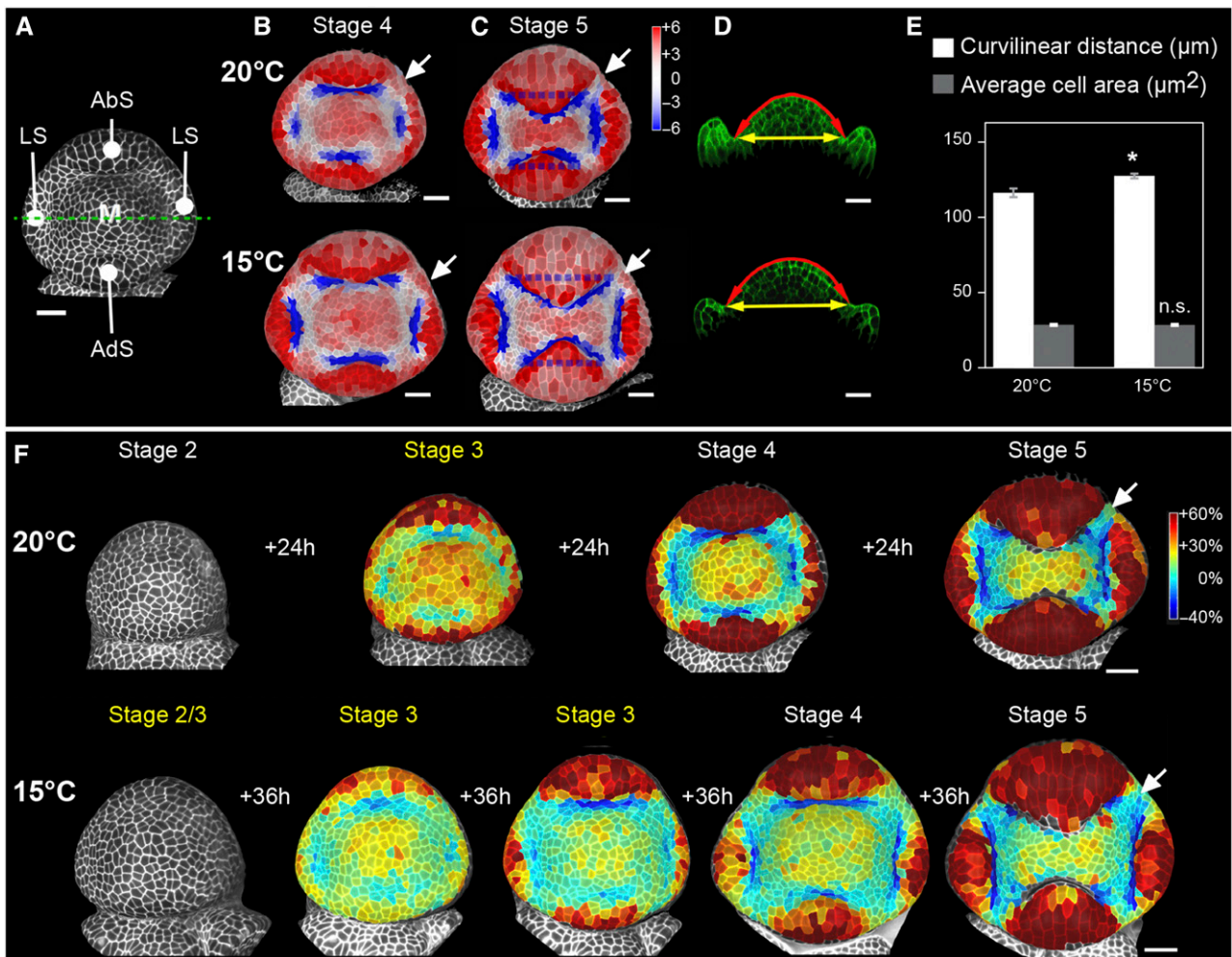
Ambient Temperature Affects Petal Number via Growth and Maturation of the Floral Bud

To investigate how ambient temperature affects petal number, we quantified the progression of shape and size of floral buds during early stages of floral development in time-lapse images of *C. hirsuta* plants grown at 15°C and 20°C (Fig. 4A; Supplemental Figs. S5 and S6). By computing local curvature with the 3D image analysis software MorphoGraphX (Barbier de Reuille et al., 2015), we found that the shape of floral buds differed between temperatures (Fig. 4, B and C). In stage 4 flowers, flat regions formed between the sepals

Figure 3. Petal number in *C. hirsuta* responds to photoperiod, ambient temperature, light quality, and vernalization. A and B, Box plots compare petal number per flower between different photoperiods, ambient temperature, and light quality (A), and in response to vernalization at ~4°C (B). C and D, Average petal number per flower over successive floral nodes in response to ambient temperature (C) and to photoperiod (D); the first floral node is labeled as 1; error bars show SE. Petals/flower are scored in the first 25 floral nodes in A and B. Pairwise comparisons by Mann-Whitney *U* test. Significance levels: ***P < 0.001, **P < 0.01, *P < 0.05. ND, Neutral days (12:12); SD, short days (8:16); LD, long days (16:8); WL, white light; BL, blue light; FRL, far-red light. *n* = 26–28 (ND, 20°C, WL); *n* = 7–26 (LD, 20°C, WL); *n* = 26–29 (SD, 20°C, WL); *n* = 12–31 (ND, 15°C, WL); *n* = 29–31 (ND, 20°C, FRL); *n* = 22–31 (ND, 20°C, BL); *n* = 12 (vernalization). Box plots show 25th to 75th percentiles, whiskers extend down to 10th and up to 90th percentiles, black line shows median, and red line shows mean.

Figure 4. Ambient temperature affects the size of intersepal regions in *C. hirsuta* floral buds. A, Early floral development in *C. hirsuta* was staged by the size and shape of sepals according to Supplemental Table S2. M, Floral meristem; LS lateral sepals; AbS, abaxial sepal; AdS, adaxial sepal. All subsequent floral buds are oriented this way. Green dashed line indicates position of optical sections shown in D. B and C, Local curvature computed with MorphoGraphX software in stage 4 (B) and stage 5 (C) floral buds of *C. hirsuta* at 20°C (top) and 15°C (bottom). Heat map indicates tissue curvature in $10^{-2} \mu m^{-1}$, where flat is white, negative curvature is blue, and positive curvature is red. Arrows indicate flat regions between sepals. Dashed blue lines approximate the sepal-meristem boundaries when these are obstructed by sepal growth in C. D, Optical cross sections of stage 4 floral buds of *C. hirsuta* at 20°C (top) and 15°C (bottom). Two measures of floral meristem size are indicated: the direct distance (yellow arrow) and the curvilinear distance (red arrow) between lateral sepal boundaries. E, Bar plot of curvilinear distance across the floral meristem (white) and epidermal cell area in the floral meristem (gray) of stage 4 floral buds of *C. hirsuta* at 20°C and 15°C. Curvilinear distance is significantly different between temperatures ($P = 0.02$; Student's *t* test). F, Areal growth computed with MorphoGraphX software in time-lapse series of *C. hirsuta* floral buds at 20°C (top) and 15°C (bottom). Arrows indicate regions of slower growth between sepals. Heat map indicates cell areal growth in percentage over intervals of 24 h (20°C, top) or 36 h (15°C, bottom). Stage 3 is marked in yellow to highlight the considerable delay in development through this stage at 15°C. Note the 15°C series is composed of two different time-lapse series (Supplemental Fig. S11), and the heat map is saturated for high growth in the sepals in order to discriminate between growth in the floral meristem and intersepal regions. Scale bars = 20 μm.

(arrows, Fig. 4B) as boundaries developed between the growing sepals and the meristem (in blue, Fig. 4B). These intersepal regions were wider in flowers grown at 15°C than at 20°C (arrows, Fig. 4B). During stage 5, as the boundaries separating sepals from the meristem extended, the intersepal regions narrowed considerably in flowers grown in 20°C, whereas at 15°C, these regions remained wider (arrows, Fig. 4C).

The size of the floral bud was also larger in plants grown at 15°C than at 20°C. For example, floral meristem area was larger in stage 4 flowers grown at 15°C ($6597 \mu m^2 \pm 135$, $n = 3$) than at 20°C ($5748 \mu m^2 \pm 16$, $n = 3$, $P < 0.05$, Student's *t* test), and the distance across the meristem was larger in 15°C- than 20°C-grown flowers (Fig. 4, D and E; Supplemental Fig. S8; Supplemental Table S5). This difference in meristem

size did not correspond to an increase in cell size but rather to an increase in cell number in flowers grown at 15°C compared to 20°C (Fig. 4E; Supplemental Fig. S8). At stage 2, prior to floral organ formation, floral buds were already significantly larger in plants grown at 15°C compared to 20°C but had a similar shape (Supplemental Fig. S9). Therefore, cool ambient temperature increased the size of *C. hirsuta* floral buds prior to the change in shape that emerged as sepals grew out.
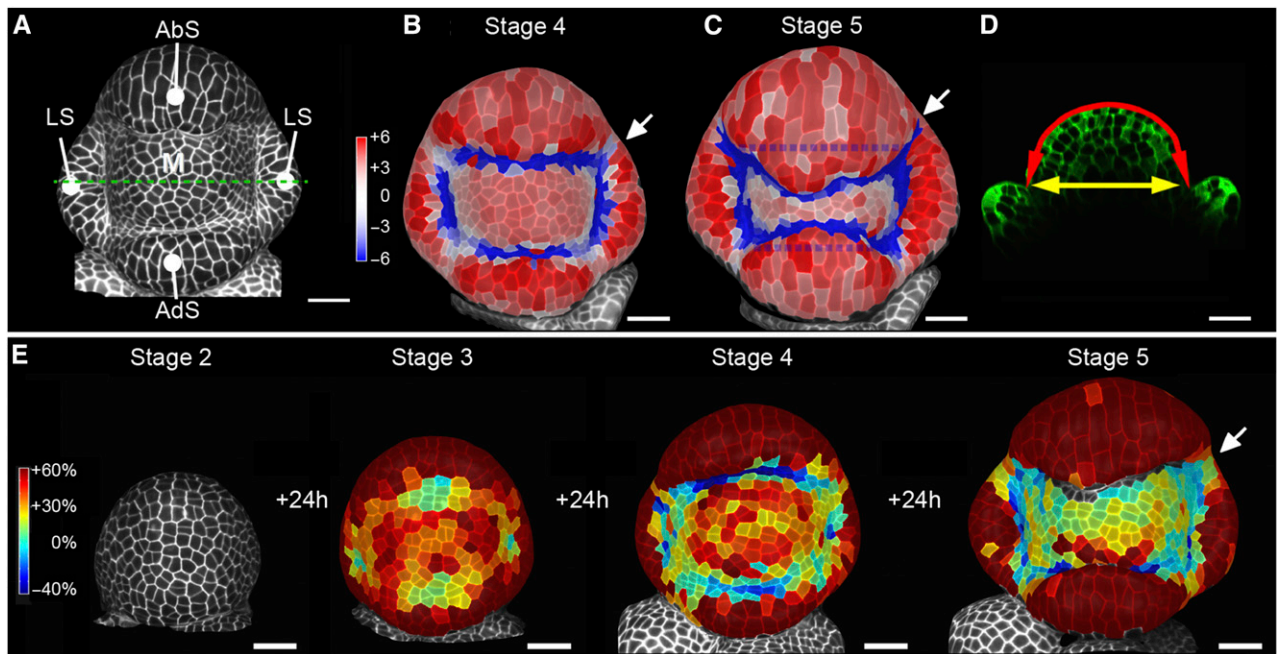
To investigate how larger intersepal regions were produced in floral buds at cooler ambient temperatures, we analyzed growth using time-lapse images of *C. hirsuta* plants grown at 15°C and 20°C. By computing areal growth with MorphoGraphX software (Barbier de Reuille et al., 2015), we found that the wider intersepal regions at 15°C did not arise from rapid, local growth of these regions that would "push" sepals apart. Instead, we found that intersepal regions were slow growing (arrows in Fig. 4F), with growth rates more similar to the meristem flanks than the fast-growing sepals (Fig. 4F). Furthermore, the rate at which floral buds matured through successive developmental stages was considerably slower at 15°C compared to 20°C: Flowers grown at 20°C took 72 h to transition through stages 2 to 5, whereas this same transition took approximately 144 h in flowers grown at 15°C (Fig. 4F; Supplemental Figs. S6, S7, and S10). This delay was particularly pronounced during stage 3, when the floral bud was enlarging but before the sepals became separated from the meristem by boundaries (stages highlighted in yellow, Fig. 4F). This delayed development was reflected in the slower growth of sepals at 15°C than at 20°C, which was slowed down more than meristem growth by cool ambient temperature (Supplemental Fig. S10). The meristem also grew for longer at 15°C before sepals started to grow rapidly at stage 4, resulting in a larger floral meristem (Fig. 4F). Thus, both a slower rate of sepal growth and an extended phase of meristem enlargement contributed to the difference in flower bud shape between 15°C and 20°C. In effect, since sepals did not increase in size as much as the meristem at 15°C, the sepal boundaries did not completely separate the meristem from whorl 1, leaving wide, flat regions between sepals in stage 5 flowers (arrows, Fig. 4, C and F). Since wider intersepal regions were associated with more petals in flowers grown at 15°C than 20°C (15°C, mean = 3.3 ± 0.1, $n = 208$; 20°C, mean = 1.6 ± 0.1, $n = 210$, $P < 0.001$, Mann-Whitney U test), these regions are likely important for petal initiation in *C. hirsuta*.

To understand whether the development of *C. hirsuta* flowers grown at 15°C resembled Arabidopsis flowers, we analyzed early stages of floral development in time-lapse images of Arabidopsis plants grown at 20°C (Fig. 5A; Supplemental Fig. S7). This comparison revealed considerable divergence in the development of four-petaled flowers between species. For example, when we computed local curvature (Barbier de Reuille et al., 2015), we found a critical difference in shape between floral buds of *C. hirsuta* and Arabidopsis. At stage 4, the floral meristem of Arabidopsis was clearly separated from the first whorl by sepal boundaries (in blue, Fig. 5B). The sepal boundaries were connected at stage 5 (Fig. 5C), leaving no flat regions between sepals like the ones observed in *C. hirsuta* (Fig. 4C). Furthermore, the curved distance across stage 4 floral meristems was more similar between Arabidopsis (117.5 μm ± 1.5, $n = 4$) and *C. hirsuta* at 20°C (115 μm ± 2.8, $n = 4$), even though their petal number differed, than *C. hirsuta* at 15°C (125 μm ± 1.5, $n = 4$; red arrow, Fig. 5D; Supplemental Table S5). We used the ratio of curvilinear/direct distance to measure meristem curvature (Fig. 5D) and found that the Arabidopsis meristem is more curved (ratio = 1.6, $n = 4$) than *C. hirsuta* (ratio = 1.3, $n = 4$ at 20°C and $n = 4$ at 15°C; Supplemental Table S5). By analyzing areal growth (Barbier de Reuille et al., 2015), we found broadly similar growth patterns between Arabidopsis and *C. hirsuta* flowers (Figs. 5E and 4F; Supplemental Fig. S5). However, regions of slower growth between sepals (arrow, Figure 5E), which influence petal initiation in Arabidopsis (Lampugnani et al., 2012), formed after the sepal boundaries completely separated the meristem from the first whorl (in blue, Fig. 5, B and C). Therefore, the intersepal regions in Arabidopsis are not flat and are physically separated from the floral meristem by boundary cells with negative curvature (Fig. 5, B and C). Whereas in *C. hirsuta*, the boundaries that physically separate each sepal from the floral meristem are discontinuous, leaving flat intersepal regions that connect the meristem with the first whorl (Fig. 4, B and C). In summary, we found no association between petal number and geometry or size of the floral bud when comparing between species.

Environmental Factors Influence Age-Dependent Variation in Sepal Trichome Number

The number of trichomes on the abaxial surface of sepals varies in an age-dependent manner, similar to the variation in *C. hirsuta* petal number (Pieper et al., 2016). In fact, the decline in sepal trichomes and petals is strongly correlated (Fig. 6A), and QTL analysis has shown that these age-dependent traits share a common genetic basis (Pieper et al., 2016). To investigate whether sepal trichome number responded to environmental variation in a similar manner to petal number, we counted sepal trichomes in the same experiments where we measured flowering time and petal number (Supplemental Table S3). We found that plants grown in short days developed significantly more sepal trichomes per flower than either neutral-day- or long-day-grown plants ($P < 0.001$, Mann-Whitney U test; Fig. 6B), and this response to photoperiod was positively correlated with petal number ($r = 0.72$, Pearson coefficient of correlation, $P < 0.001$). Plants grown at 15°C also developed more sepal trichomes per flower than those grown at 20°C ($P < 0.001$, Mann-Whitney U test; Fig. 6B), and this response also showed a strong positive correlation with petal number ($r = 0.91$, Pearson coefficient of correlation,

Figure 5. Geometry of the intersepal regions in Arabidopsis floral buds differs from *C. hirsuta*. A, Early floral development in Arabidopsis was staged by the size and shape of sepals according to Smyth et al. (1990). M, Floral meristem; LS, lateral sepals; AbS, abaxial sepal; AdS, adaxial sepal. All subsequent floral buds are oriented this way. Green dashed line indicates position of optical section shown in D. B and C, Local curvature computed with MorphoGraphX software in stage 4 (B) and stage 5 (C) floral buds of Arabidopsis at 20°C. Heat map indicates tissue curvature in 10^{-2} $\mu\mathrm{m}^{-1}$, where flat is white, negative curvature is blue, and positive curvature is red. Arrows indicate intersepal regions. Dashed blue lines approximate the sepal-meristem boundaries when these are obstructed by sepal growth in C. D, Optical cross section of stage 4 floral bud showing two measures of floral meristem size: the direct distance (yellow arrow) and the curvilinear distance (red arrow) between lateral sepal boundaries. E, Areal growth computed with MorphoGraphX software in time-lapse series of Arabidopsis floral buds at 20°C. Arrow indicates intersepal region with slower growth. Heat map indicates cell areal growth in percentage over intervals of 24 h. Note the heat map is saturated for high growth in the sepals in order to discriminate between growth in the floral meristem and intersepal regions. Scale bars = 20 μm.

$P < 0.001$). The one exception to this trend was the reduction in sepal trichomes in plants grown in far-red light, compared to white or blue light ($P < 0.05$, Tukey Kramer; Fig. 6B; Supplemental Fig. S4), which was not correlated with petal number.

To understand whether the correlated response of petal and sepal trichome number to environmental variation reflected a common, age-dependent response of both traits, we assessed the average number of sepal trichomes at individual floral nodes. In comparison to petals (Fig. 3C), we found that sepal trichome number was high in the first floral nodes in plants grown at 15°C compared to 20°C and declined sharply (Fig. 6C). Growth in short-day conditions affected the number of sepal trichomes in a similar way as petals: high in the first floral nodes before declining (Figs. 3D and 6D). Therefore, petal and sepal trichome number share an age-dependent trend in their response to environmental variation.
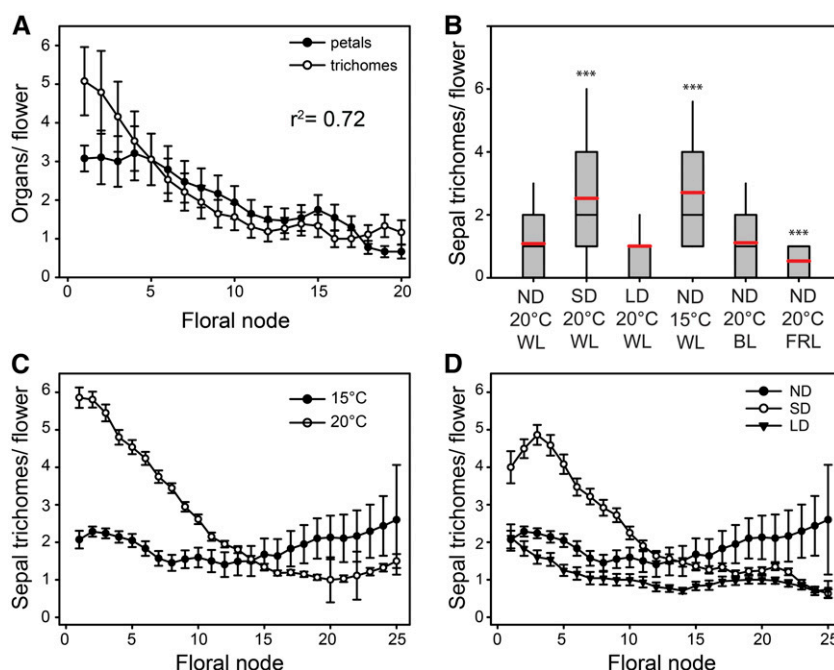
Petal Number Regulation by Endogenous Signals

To investigate whether the endogenous ageing pathway may contribute to the observed trend in petal number variation, we assessed petal number in *C. hirsuta*

genotypes with accelerated ageing. The abundance of *SPL* transcripts regulates ageing in Arabidopsis and is determined by the declining levels of miR156 throughout a plant's life (Wang et al., 2009; Wu et al., 2009). To get an overview of *SPL* expression changes during the transition from vegetative to floral development in *C. hirsuta*, we examined transcript levels of *ChSPL3*, *ChSPL15*, and *ChSPL9* (Fig. 7A), which represent three subgroups of miRNA-regulated *SPL* genes (Guo et al., 2008). These genes were also chosen because they contribute to the regulation of sepal trichome number in Arabidopsis (Shikata et al., 2009; Yu et al., 2010; Wei et al., 2012). We found that *ChSPL3* expression increased stepwise from vegetative to early inflorescence to anthesis stages of development, while *ChSPL9* expression increased from early inflorescence to anthesis stages (Fig. 7A). *ChSPL15* expression increased between vegetative and early inflorescence stages (Fig. 7A), as had been shown previously (Cartolano et al., 2015), indicating that the expression level of all three *SPL* genes increased during ageing in *C. hirsuta*.

To assess the contribution of SPL activity to petal number variation in *C. hirsuta*, we generated transgenic

Figure 6. Variation in petal number is correlated with sepal trichomes in *C. hirsuta*. A, Average petal number (black circles) and sepal trichome number (white circles) over consecutive floral nodes are correlated (R^2 = 0.72); the first floral node is labeled as 1. B, Box plot compares sepal trichome number per flower between different photoperiods, ambient temperature, and light quality. C and D, Average sepal trichome number per flower over successive floral nodes in response to ambient temperature (C) and to photoperiod (D). Sepal trichomes/flower are averaged over the first 25 floral nodes in B. Pairwise comparisons by Mann-Whitney *U* test. Significance levels: ***$P <$ 0.001, **$P <$ 0.01, *$P <$ 0.05. ND, Neutral days (12:12); SD, short days (8:16); LD, long days (16:8); WL, white light; BL, blue light; FRL, far-red light. n = 26–28 (ND, 20°C, WL); n = 7–26 (LD, 20°C, WL); n = 26–29 (SD, 20°C, WL); n = 12–31 (ND, 15°C, WL); n = 29–31 (ND, 20°C, FRL); n = 22–31 (ND, 20°C, BL). Error bars show SE. Box plots show 25th to 75th percentiles, whiskers extend down to 10th and up to 90th percentiles, black line shows median, and red line shows mean.
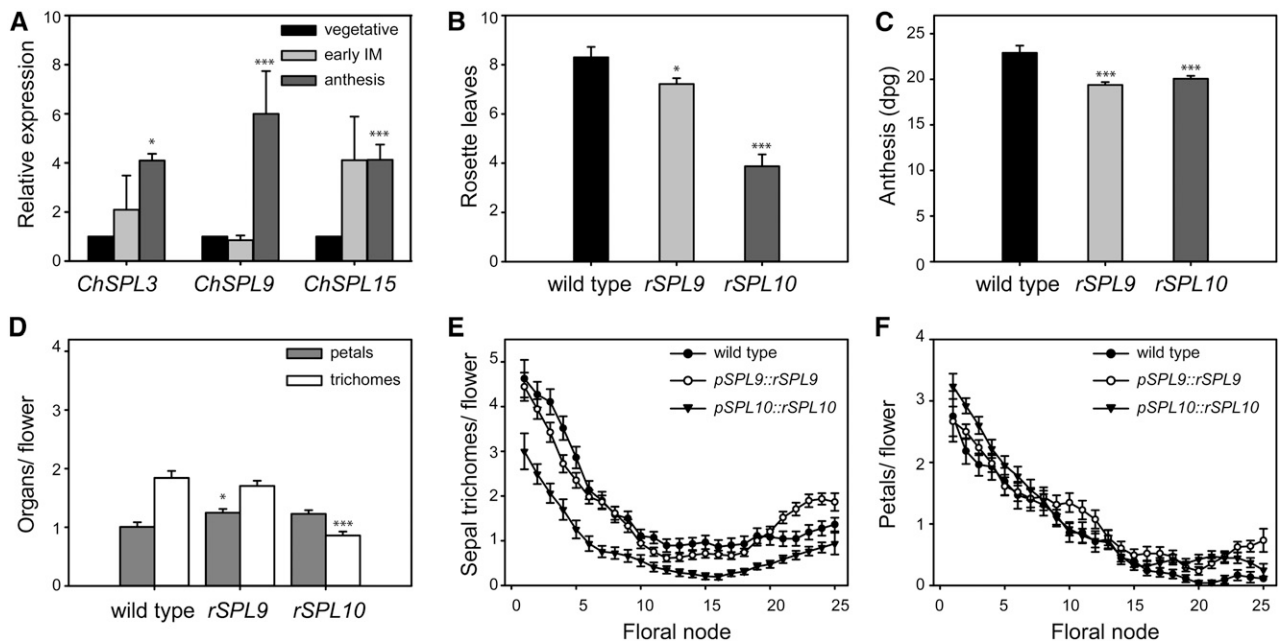

plants expressing miRNA-resistant versions of the Arabidopsis genes *SPL9* and *SPL10* (*pSPL9::rSPL9*, *pSPL10::rSPL10*; Wu et al., 2009). We found that flowering time was accelerated in these miRNA-resistant plants compared to wild type (Supplemental Table S6), as measured by a reduction in rosette leaf number (Fig. 7B) and days to anthesis (Fig. 7C). We also found a reduced number of sepal trichomes in *pSPL10::rSPL10* plants (Fig. 7, D and E; Supplemental Table S6), which agrees with the repression of sepal trichomes by *SPL10* in Arabidopsis (Shikata et al., 2009). However, we still observed a temporal trend in the decline of sepal trichomes in *pSPL10::rSPL10* plants (Fig. 7E), suggesting that additional factors contribute to this age-dependent process in these plants. Taken together, these results indicate that ageing is accelerated by the transgenic expression of miRNA-resistant SPLs in *C. hirsuta*, particularly in *pSPL10::rSPL10* plants. However, average petal number per flower was not different between these transgenic lines and wild type (Fig. 7, D and F; Supplemental Table S6) and furthermore, each genotype showed the same decline in petal number during plant ageing (Fig. 7F), suggesting that petal number variation is insensitive to the accelerated ageing caused by the expression of miRNA-resistant *SPL9* and *SPL10* in *C. hirsuta*.

The growth hormone GA is another endogenous signal that promotes flowering in Arabidopsis (Eriksson et al., 2006; Andrés et al., 2014). To investigate whether *C. hirsuta* petal number varies in response to GA levels, we treated *C. hirsuta* with 0, 0.1, or 10 μM GA$_3$. First, we measured how flowering time in *C. hirsuta* responded to these increasing GA$_3$ levels under neutral day (12 h:12 h light/dark) conditions. We found that flowering time was accelerated by increasing concentrations of GA$_3$,

with the number of rosette leaves and the time to visible floral buds decreasing with progressive GA$_3$ dose (Fig. 8A; Supplemental Table S7). We also observed an increase in cauline leaf number in response to 10 μM GA$_3$, which likely reflected an acceleration of the reproductive transition such that cauline leaves are produced at the shoot apical meristem instead of rosette leaves (Fig. 8A). Therefore, elevated GA levels promote flowering in *C. hirsuta*. Although the average number of petals per flower was unaltered in neutral-day conditions, we found a clear dose response under long days (16 h:8 h light/dark), with petal number steadily increasing in response to increasing concentrations of GA$_3$ (Fig. 8B; Supplemental Fig. S6). In contrast to the dose response of petal number to GA, the production of sepal trichomes was strongly inhibited by 10 μM GA$_3$ application in both long days and neutral days (Fig. 8B), similar to Arabidopsis (Gan et al., 2007). Therefore, our results suggest that petal number variation in *C. hirsuta* responds to GA during photoperiodic flowering.

DISCUSSION

The number of petals produced in *C. hirsuta* flowers shows seasonal variation. Flowers produce more petals in spring than in summer. Our findings indicate that the cool ambient temperatures associated with spring flowering have a considerable effect on petal number. Growth at cool temperature extended the time interval during which floral buds matured in *C. hirsuta*. In particular, an extended phase of meristem formation and slow sepal growth at 15°C compared to 20°C, produced larger floral buds with wide, flat regions between sepals. Petal number varied in response to

Figure 7. Petal number variation is insensitive to accelerated ageing in *C. hirsuta*. A, Relative expression of *ChSPL3*, *ChSPL9*, and *ChSPL15* transcripts in vegetative SAM (black), early IM with 5 to 10 floral buds (light gray), and IM at anthesis (dark gray). Pairwise differences in expression are significant for *ChSPL3* between early IM and anthesis, and for *ChSPL9/15* between vegetative SAM and anthesis. B and C, Flowering time, measured by rosette leaf number (B) and time to anthesis (C) in transgenic lines expressing miRNA-resistant versions of *SPL9* and *SPL10*. D, Average petal number per flower (gray) and sepal trichomes per flower (white) in *pSPL9:rSPL9* and *pSPL10:rSPL10* lines. E, Average sepal trichome number per flower is lower in all floral nodes in *pSPL10:rSPL10* lines. F, Average petal number per flower is similar at successive floral nodes in wild-type, *pSPL9::rSPL9*, and *pSPL10:rSPL10* plants. Pairwise comparisons by Mann-Whitney U test. Significance levels: ***$P < 0.001$, **$P < 0.01$, *$P < 0.05$. Petals and sepal trichomes/flower are averages of the first 25 floral nodes. Error bars show SE.

numerous other external and endogenous cues, including photoperiod, simulated shade, vernalization, and GA levels. Underlying this variation was a temporal decline in petal number during plant ageing; however, this trend was unaffected by the accelerated ageing imposed by miRNA-resistant *SPL9* or *SPL10* expression. In summary, petal number is a quantitative trait in *C. hirsuta* with a complex genetic architecture (Pieper et al., 2016) that responds to environmental variation.

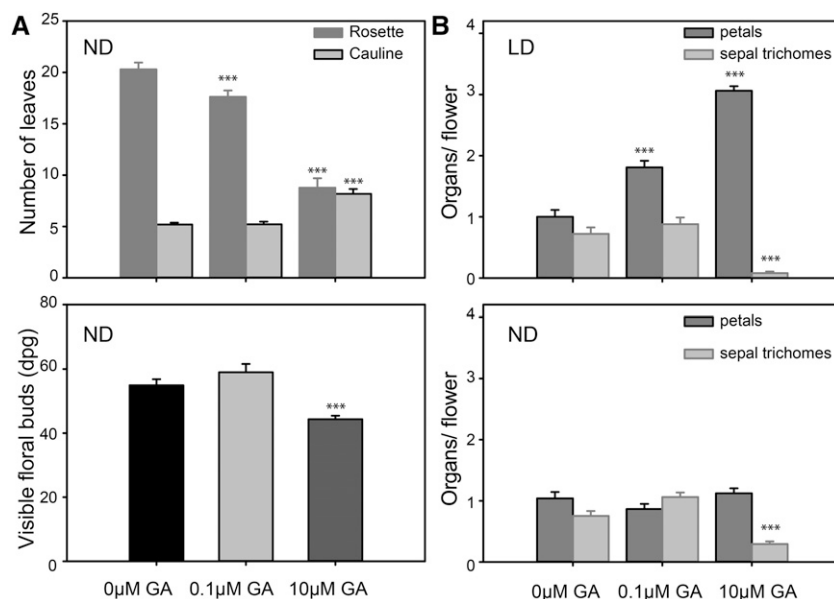## Developmental Basis for Ambient Temperature Effect on Petal Number

In Arabidopsis, and most other plants, a predictable number of petals develop in each flower. This robustness is lost in *C. hirsuta*, resulting in a variable number of petals per flower (Monniaux et al., 2016; Pieper et al., 2016). We have shown that this phenotype is influenced by both genetic variation (Pieper et al., 2016) and here, by environmental variation. Through a quantitative analysis of early floral development at 15°C compared to 20°C, we discovered that growth at cooler temperatures extends the maturation of floral primordia over a longer time in *C. hirsuta*. Slower maturation of the floral bud increases the size of the floral meristem prior to sepal growth and, coupled with a slower rate of sepal

growth, results in wide, flat regions between sepals that are associated with the formation of more petals per flower. Work in Arabidopsis has described a feed-forward loop that regulates the onset of flower differentiation at stage 3 and positive-feedback loops that stably maintain this regulatory module (Liu et al., 2009; Wagner, 2009). This temporal regulation ensures that the proliferative phase of floral meristem formation is completed before flower differentiation begins at stage 3, in order to support the formation of the correct number of floral organs. Our findings suggest that in *C. hirsuta*, ambient temperature may provide input to this regulatory module, such that floral meristem maturation becomes more gradual at 15°C. Alternatively, ambient temperature may be integrated by the canonical WUS-CLV system to control floral stem cell number and proliferation. However, it is important to note that only petal number varies in response to temperature in *C. hirsuta*, indicating that the change in floral meristem size is not sufficient to elicit a general increase in floral organ numbers (Clark et al., 1993, 1995; Running et al., 1998; Fletcher, 2001). These observations suggest that petal initiation in *C. hirsuta* is particularly sensitive to the space available between sepals in the developing floral bud.

The genetic regulation of intersepal regions and their role in petal initiation have previously been investigated in Arabidopsis. The trihelix transcription factor

Figure 8. Petal number in *C. hirsuta* responds to elevated GA during long-day photoperiods. A, Flowering time, measured by rosette (dark gray), and cauline (light gray) leaf number, and number of days after germination when the first floral buds are visible, responds to increasing GA₃ concentrations (0, 0.1, and 10 μM) in ND. B, Average number of petals per flower (dark gray) responds to increasing GA₃ concentrations (0, 0.1, and 10 μM) in LD but not ND. Sepal trichome number (light gray) was decreased by 10 μM GA₃ treatment in LD and ND. Multiple comparisons by Kruskal-Wallis test with post hoc analysis using the Tukey Kramer method. Significance levels: ***$P <$ 0.001, **$P <$ 0.01, *$P <$ 0.05. ND, neutral days (12:12); LD, long days (16:8). Petals and sepal trichomes/flower are averages of the first 25 floral nodes. Error bars show SE.

gene *PTL* is expressed in intersepal regions, and *ptl* mutants show variable petal loss (Griffith et al., 1999; Brewer et al., 2004). Petal initiation is thought to be disrupted in *ptl* mutants as a consequence of growth distortions in the intersepal regions, which influence auxin accumulation in adjacent regions of the floral meristem where petals initiate (Lampugnani et al., 2012, 2013). Therefore, PTL regulates the size of the intersepal regions and indirectly regulates petal number. *CUP-SHAPED COTYLEDON* transcription factor genes also regulate the size of the intersepal regions, and therefore petal number, by inhibiting the growth of sepal tissues in the intersepal regions (Laufs et al., 2004; Mallory et al., 2004; Baker et al., 2005; Lampugnani et al., 2012). In this way, gain or loss of petals is due to larger or smaller boundaries between sepals. This process captures a common developmental logic for auxin-mediated organ outgrowth that was previously incorporated in computational models of phyllotaxis and leaf serration (Smith et al., 2006; Bilsborough et al., 2011). Therefore, similar modeling approaches are likely to inform our understanding of the mechanism of petal initiation.

We have also shown here that it is important to consider the three-dimensional shape and local curvature of floral buds and how space emerges between sepals via growth. The intersepal regions of Arabidopsis and *C. hirsuta* floral buds have very different geometries. In Arabidopsis, the sepal whorl is completely separated from the floral meristem by boundary cells with negative curvature. Whereas in *C. hirsuta*, the boundaries that separate sepals and meristem are discontinuous, leaving the intersepal regions connected to the meristem. Growth at cool temperatures increases the size of these intersepal regions with an associated increase in petal number per flower. One possibility is that this larger intersepal space allows enough auxin to accumulate in the adjacent floral meristem to drive petal outgrowth. However, this remains to be tested. Moreover, we showed that petal number varied in response to other external and endogenous cues, in addition to ambient temperature, suggesting that petal initiation in *C. hirsuta* may be influenced by multiple different developmental paths.

Flowering Time and Petal Number Variation in *C. hirsuta*

Our findings show that flowering time in *C. hirsuta* is mostly sensitive to the same environmental and endogenous factors that are known to regulate Arabidopsis flowering. Lengthened photoperiods accelerated flowering time, as did vernalization, far-red enriched light, increased GA levels, and precocious ageing caused by miRNA-resistant *SPL9* or *SPL10* expression. In contrast to Arabidopsis, cooler ambient temperatures of 15°C accelerated flowering time, but this may be a mild vernalization effect caused by extended periods of vegetative growth at cool temperatures under neutral days. Blue enriched light failed to elicit a flowering time response in *C. hirsuta* in neutral days, although we cannot exclude that plants may be more responsive under long days. Flowering time is a quantitative trait, and *FLC* was identified as a major QTL controlling this trait in both *C. hirsuta* (Cartolano et al., 2015) and Arabidopsis (Koornneef et al., 1994; Lee et al., 1994; Michaels and Amasino, 1999). Here, we defined the plastic response of flowering time in the early flowering Ox accession of *C. hirsuta* to numerous different cues. It will be interesting to characterize the flowering response of other *C. hirsuta* accessions, particularly late-flowering accessions, to these same cues, and to further understand the genetic basis of flowering time in *C. hirsuta*.

We found that petal number in *C. hirsuta* varied in response to many of the same environmental and endogenous factors that regulated flowering. However, petal number and flowering time did not precisely covary in response to the same cues. For example, we defined five conditions that significantly increased petal number: cool temperature, short photoperiod, simulated shade, vernalization, and elevated GA levels. Although flowering time was accelerated in most of these conditions, it was significantly delayed in short days. Therefore, early flowering did not strictly associate with more petals per flower. Moreover, at least 15 QTL have been detected where natural allelic variation affected petal number in *C. hirsuta*, and few of these colocated with flowering time QTL (Cartolano et al., 2015; Pieper et al., 2016). Interpreting our results in the context of seasonal variation, we suggest that certain environmental conditions associated with spring flowering in our field experiments, such as cool daily temperatures and extended vernalization, may act together to promote petal formation.

Regulation of Petal Number by Endogenous Pathways

Petal number declined during the ageing of *C. hirsuta* plants in both field and greenhouse settings, and this trend was apparent under all environmental conditions tested. In conditions where petal number was increased, such as spring field conditions, cool temperatures, or short days, petal number was higher in the first flowers produced and continued to stay high over a longer period of flower production before declining. This suggests that the inhibitory effect of ageing on petal formation was delayed in these conditions. This temporal trend in petal number was strongly correlated with a decline in the number of trichomes on the sepals of successive flowers. Using QTL analysis, we had previously shown that these two traits share a common genetic basis in *C. hirsuta* (Pieper et al., 2016). Similar to Arabidopsis, we found that *SPL* gene expression increased during ageing in *C. hirsuta*, and ageing was accelerated by expressing artificial microRNA-resistant versions of *SPL9* or *SPL10*, indicated by accelerated flowering time and a further decline in sepal trichome number. Yet petal number was insensitive to accelerated ageing in these genotypes, suggesting that petal number is not regulated by the age-sensing pathway comprised of miR156 and its targets in the *SPL* gene family. However, it is clear that individual *SPL* genes have specific roles in different developmental transitions that lead to flower formation in Arabidopsis (Yamaguchi et al., 2014; Hyun et al., 2016). Therefore, a comprehensive analysis of *SPL* gene function in *C. hirsuta* is required to fully understand the contribution of this ageing pathway to petal number variation.

The level of GA is another endogenous signal that influences flowering in Arabidopsis, and we found a dose-dependent acceleration of flowering and increase of petal number in *C. hirsuta* in response to GA. Specifically,

we found that a long-day photoperiod was necessary to elicit this increase in petal number, as GA application had no effect on petal number in neutral days. GA biosynthesis is known to be regulated by the photoperiod pathway. In long days, *SVP* expression falls and contributes to increasing the levels of GA, which accelerates flowering by promoting *SPL* gene transcription (Andrés et al., 2014). Our results indicate that *C. hirsuta* petal number increases in response to GA application under these long-day conditions. Moreover, GA regulates SPL activity by promoting the degradation of DELLA repressors and thereby releasing SPL transcription factors to activate floral-promoting MADS-box genes in Arabidopsis (Yu et al., 2012). Therefore, the endogenous signals provided by the age of a plant and its GA levels are likely to be connected at a molecular level and influence the number of petals formed in each *C. hirsuta* flower.

Petal Number Plasticity

To find seasonal variation in a robust trait like petal number is unusual. Flowers usually form a predictable number of floral organs, and this regularity forms the basis of many taxonomic classifications. For example, crucifers take their name from the cross shape of their four petals. Flowers acquired a stable number of organs, of defined identity, via the canalization of floral development pathways during angiosperm evolution (Specht and Bartlett, 2009). A strong driver of this canalization was likely to be the recognition of predictable floral morphologies by pollinators. Therefore, it is interesting to speculate about what factors might maintain the derived trait of petal number variation in *C. hirsuta*.

One factor is the polygenic architecture that controls petal number in *C. hirsuta*. Small to medium effect alleles at many loci act to increase and decrease petal number in *C. hirsuta*, thus maintaining a variable petal number below four (Pieper et al., 2016). Induced alleles of large effect can shift petal number close to four and reduce variability, but natural alleles of this effect were not detected in five different recombinant inbred line populations (Pieper et al., 2016). Another factor is the selfing habit of *C. hirsuta* (Hay et al., 2014). Floral traits often evolve as part of a selfing syndrome because the selective pressure to attract pollinators is relaxed (Sicard and Lenhard, 2011). Therefore, petal number may vary by drift. However, the seasonal variation that we observed in *C. hirsuta* petal number suggests that petal number may be optimized for different conditions. Given that petals assist with opening the floral bud, high petal number may be optimal in conditions that favor pollination in an open flower and provide an opportunity to outcross. Low petal number is likely to result in obligate and efficient self-pollination in the unopened floral bud and may be optimal in conditions that are less favorable for pollination in an open flower, such as warmer temperatures where the risk of dehydration is

higher. In this way, petal number plasticity could provide *C. hirsuta* with a flexible mating system that responds to environmental conditions. *C. hirsuta* has traits such as explosive seed dispersal that allow this widespread, ruderal species to successfully colonize disturbed habitats (Hofhuis et al., 2016). The uncertain pollination conditions experienced by pioneer weeds may also contribute to maintaining petal number plasticity in *C. hirsuta*.

CONCLUSION

In summary, we have shown that the maturation of floral buds is affected by ambient temperature in *C. hirsuta* and influences the flat space available between sepals in each flower. Variation in this space appears to be a limiting factor for petal formation in *C. hirsuta*, rendering the potential for each petal to initiate vulnerable to heterogeneity in floral bud maturation. We propose that environmental variation influences this heterogeneity, providing a developmental route for petal number to respond plastically to seasonal conditions.

MATERIALS AND METHODS

Plant Material and Transgenic Plant Construction

Wild-type *Cardamine hirsuta* used in this study was the Oxford (Ox) accession (specimen voucher Hay 1 [OXF]; Hay and Tsiantis, 2006). Seeds were sown onto a moistened mix of 1:1 mix John Innes No. 3 compost and vermiculite. For all treatments, seeds were stratified for 7 d at 4°C and then moved into Snijders growth cabinets illuminated with cool-white fluorescent tubes at 50 μmol m^{-2} s^{-1} unless otherwise indicated. To analyze wild-type and transgenic plant development, plants were grown in greenhouses at 16 h light (22°C), 8 h dark (20°C), unless otherwise indicated. Local stands of *C. hirsuta* in Oxford, UK, were scored for petal number in March/April (spring flowering) and July/August (summer flowering) 2011. *SPL9pro::rSPL* and *SPL10pro::rSPL10* plasmids (gift from S. Poethig; Wu et al., 2009) were transformed into *C. hirsuta* by *Agrobacterium tumefaciens*-mediated floral dip ,and at least 10 independent lines were generated for each construct.

Field Experiments

Field studies were conducted at the MPIPZ, Cologne, Germany in April/May 2016 (spring) and August 2016 (summer), using the Ox accession. The field was prepared by clearing weeds, watering soil, and dividing it into equal plots. For the spring experiment, seeds were stratified at 4°C for 1 week and sown on sterile Jiffy-7 peat pellets. Seedlings were grown for about 4 weeks in a greenhouse without temperature or light control, and whole peat pellets were planted in the field. For the summer experiment, seeds were surface-sterilized, sown on 0.5× Murashige and Skoog medium plates and stratified for 1 week. Seeds were left to germinate for 1 week in a growth chamber under standard conditions, then seedlings were transferred to sterile Jiffy-7 peat pellets and grown in a greenhouse without temperature or light control for 3 weeks, and whole peat pellets were planted in the field where plants were watered regularly.

Photoperiod, Ambient Temperature, and Light Quality Treatments

Photoperiod: Plants were grown at 20°C under white light in either long days (LD; 16 h light:8 h dark), neutral days (ND; 12 h light:12 h dark), or short days (SD; 8 h light:16 h dark). Temperature: Plants were grown at 20°C and 15°C under white light in neutral days. Light quality: Plants were grown at 20°C in neutral days in far-red-enriched light. The red light (630–690 nm) to far-red light

(700–760 nm) ratio was 1.10 ± 0.02 (SE) in white light. We supplemented this with far-red light from a GreenPower LED module HF far red (Trilight) to yield a red:far-red light ratio of 0.45. Plants were also grown at 20°C in neutral days in blue-enriched light. In white light, the ratio of blue to total wavelengths was 0.14. We supplemented this with blue light from a GreenPower LED module HF blue (Trilight) to yield a ratio of blue to total wavelengths of 0.38. Total fluence was kept constant in all conditions at 35 to 45 μmol m^{-2} s^{-1}. Spectral quality and intensity was measured with an Ocean Optics spectrophotometer and OOIBase 32 software.

Photoinductive Shifts

Plants were grown for 3 weeks in moderately short-day conditions (10 h:14 h light/dark) and then moved into long-day conditions (16 h:8 h light/dark). Shoot apices were dissected and processed for scanning electron microscopy at days 4, 5, 6, 7, 8, 11, 13, 17, and 20 following the light shift. The total number of floral buds produced at each apex was counted at each sampling.

Vernalization Treatments

After germination, the majority of plants were shifted to a 4°C cold room with fluorescent lights. Equal numbers of plants were shifted back to the greenhouse after 1, 2, 3, and 4 weeks of growth at 4°C.

GA Treatments

A stock solution of 100 μM GA$_3$ (Sigma-Aldrich) was dissolved in ethanol and diluted to 0.1 or 10 μM GA$_3$ in water. Ten microliters of solution was applied to the apex of each plant 4 days after germination. Ten microliters of diluted ethanol (0 μM GA$_3$) was applied to control plants. Plants were grown in both neutral- and long-day conditions.

Scoring for Flowering Time and Petal Number

Rosette and cauline leaves were counted in mature plants. Flowering was also measured by counting the days after germination when inflorescence buds first became visible, when the primary inflorescence reached 5 cm in height, and when stamens dehisced at anthesis. The time required for visible buds to develop through to anthesis was defined as the floral maturation interval. Flowers at anthesis were removed and examined under a dissecting scope to count petal number and sepal trichome number in the first 25 flowers produced on the inflorescence. Multiple GA-treated plants arrested early and did not produce 25 nodes, so these data averages reflect all nodes carrying flowers. In the field, 10 plants were randomly chosen, their flowers at anthesis were removed every second day, and petal number was counted using a magnifying band for all flowers produced on each plant (up to 39 and 26 flowers for the spring and summer experiments, respectively).

Histology and Scanning Electron Microscopy

For semithin sections, inflorescences apices were fixed in 2.5% glutaraldehyde in phosphate buffer, dehydrated, stepwise infiltrated, and embedded in TAAB Low Viscosity resin (TAAB). Sections at 1.5 μm thickness were stained with 0.05% toluidine blue, mounted in DPX mountant (Sigma-Aldrich), and photographed. Shoot apices were prepared for scanning electron microscopy by fixation in formaldehyde:acetic acetic:ethanol, postfixed in osmium tetraoxide, dehydrated, critical point dried, and dissected before coating with gold/palladium. Samples were viewed using a JEOL JSM-5510 microscope.

RT-qPCR

Tissues were sampled at three stages: 10-d-old vegetative seedlings, early inflorescence meristems with 5 to 10 floral buds, and inflorescence apices at anthesis. RNA from three biological replicates was isolated using Qiagen's RNA easy kit. Reverse transcription cDNA synthesis was performed using the VILO cDNA synthesis kit (Invitrogen). qPCR was conducted using the Applied Biosystems 7300 Cycler. *GLYCERALDEHYDE-3-PHOSPHATE DEHYDROGENASE C SUBUNIT1* (CARHR078250) was used as an internal reference. Efficiency for primers used in qPCR was between 1.8 and 2.0. Primer sequences are listed in Supplemental Table S8. The following gene sequences can be found by these

gene identifiers in the *C. hirsuta* genome assembly: *ChAP1* (CARHR062020), *ChSVP* (CARHR113740), *ChSPL3* (CARHR127930), *ChSPL9* (CARHR137240), and *ChSPL15* (CARHR168220) (Gan et al., 2016).

Statistics

Data were tested for normality when $n < 50$ with a Shapiro Wilks test and $n > 50$ with a Lilliefores test and count data were treated as non-normally distributed. Pairwise comparisons were performed using a two-tailed Student's t test for normal data and Mann-Whitney U tests for non-normally distributed data, and the P value associated with each test was reported. Comparisons between three or more treatments were done by the Kruskal-Wallis test for non-normally distributed data, with post hoc analysis using the Tukey Kramer method at $P < 0.05$ significance level. Temporal trends were displayed using moving average smoothing. Correlations between petal and trichome number were calculated from moving average data using Pearson's r correlation coefficient. Squaring the r value (R^2) gave an estimate of the strength of the correlation. Pearson's r value was tested for significance using a critical values table at $\alpha = 0.05$ (two-tailed). REST 2009 software (V2.0.13) was used to test the statistical significance of pairwise differences in gene expression calculated from RT-qPCR data.

Time-Lapse Microscopy and Quantitative Image Analysis

Plants were grown 4 to 5 weeks on soil in long days and controlled temperature, either at 20°C (Arabidopsis [*Arabidopsis thaliana*] and *C. hirsuta*) or 15°C (*C. hirsuta*). The inflorescence was cut into segments about 5 mm long and dissected to uncover young floral primordia, then transferred to 0.5× Murashige and Skoog medium supplemented with 1.5% plant agar, 1% Suc, and 0.1% plant preservative mixture (Plant Cell Technology). To visualize cell walls, samples were stained with 0.1% propidium iodide (Sigma-Aldrich) for 2 to 5 min before each observation. Floral primordia were imaged from the top at 24-h intervals for plants grown at 20°C and 36 h for plants grown at 15°C. Live imaging was performed using a Leica SP8 upright confocal microscope equipped with a long working-distance water immersion objective (L 40×/0.8 W) and HyD hybrid detectors. Fluorescent signal of propidium iodide was collected using an argon laser at 514 nm for excitation and 600 to 660 nm for detection. Between imaging, samples were transferred to a growth cabinet and cultured in vitro in standard long-day conditions at 20°C or 15°C. To extract size, local curvature, and areal growth of floral buds, confocal time-lapse series were analyzed using MorphoGraphX software (Barbier de Reuille et al., 2015).

Supplemental Data

The following supplemental materials are available.

Supplemental Figure S1. *C. hirsuta* floral organ ontogeny.

Supplemental Figure S2. Changes in mean daily temperature and day length during spring and summer field experiments in Cologne.

Supplemental Figure S3. Different temporal measures of flowering time are correlated.

Supplemental Figure S4. Petal number in *C. hirsuta* varies during ageing and responds to light quality and vernalization.

Supplemental Figure S5. CLSM time-lapse series of early floral development in *C. hirsuta* plants grown at 20°C.

Supplemental Figure S6. CLSM time-lapse series of early floral development in *C. hirsuta* plants grown at 15°C.

Supplemental Figure S7. CLSM time-lapse series of early floral development in Arabidopsis plants grown at 20°C.

Supplemental Figure S8. Size measurements of *C. hirsuta* and Arabidopsis floral meristems.

Supplemental Figure S9. Stage 2 floral buds of *C. hirsuta* and Arabidopsis.

Supplemental Figure S10. Cell areal growth of sepals and floral meristem in *C. hirsuta* plants grown at 20°C and 15°C.

Supplemental Figure S11. Composite growth series of *C. hirsuta* plants grown at 15°C.

Supplemental Figure S12. Petal number in *C. hirsuta* varies in response to GA during long-day photoperiods.

Supplemental Table S1. Floral architecture following photoinduction in *C. hirsuta*.

Supplemental Table S2. Floral ontogeny in *C. hirsuta* following photoinduction.

Supplemental Table S3. Flowering time, petals/flower, and sepal trichomes/flower of *C. hirsuta* in response to environmental growth conditions.

Supplemental Table S4. Flowering time and petals/flower of *C. hirsuta* in response to vernalization.

Supplemental Table S5. Size measurements of *C. hirsuta* and Arabidopsis floral meristems.

Supplemental Table S6. Flowering time, petals/flower, and sepal trichomes/flower in transgenic *C. hirsuta*-expressing *miR156*-resistant constructs, *pSPL9::rSPL9*, or *pSPL10::rSPL10*.

Supplemental Table S7. Flowering time, petals/flower, and sepal trichomes/flower of *C. hirsuta* in response to gibberellin treatment.

Supplemental Table S8. Primer sequences used in study.

LITERATURE CITED

Airoldi CA, McKay M, Davies B (2015) MAF2 is regulated by temperature-dependent splicing and represses flowering at low temperatures in parallel with FLM. PLoS One **10:** e0126516

Andrés F, Coupland G (2012) The genetic basis of flowering responses to seasonal cues. Nat Rev Genet **13:** 627–639

Andrés F, Porri A, Torti S, Mateos J, Romera-Branchat M, García-Martínez JL, Fornara F, Gregis V, Kater MM, Coupland G (2014) SHORT VEGETATIVE PHASE reduces gibberellin biosynthesis at the Arabidopsis shoot apex to regulate the floral transition. Proc Natl Acad Sci USA **111:** E2760–E2769

Baker CC, Sieber P, Wellmer F, Meyerowitz EM (2005) The early extra petals1 mutant uncovers a role for microRNA miR164c in regulating petal number in Arabidopsis. Curr Biol **15:** 303–315

Barbier de Reuille P, Routier-Kierzkowska AL, Kierzkowski D, Bassel GW, Schüpbach T, Tauriello G, Bajpai N, Strauss S, Weber A, Kiss A, et al (2015) MorphoGraphX: A platform for quantifying morphogenesis in 4D. eLife **4:** 05864

Bastow R, Mylne JS, Lister C, Lippman Z, Martienssen RA, Dean C (2004) Vernalization requires epigenetic silencing of FLC by histone methylation. Nature **427:** 164–167

Bilsborough GD, Runions A, Barkoulas M, Jenkins HW, Hasson A, Galinha C, Laufs P, Hay A, Prusinkiewicz P, Tsiantis M (2011) Model for the regulation of *Arabidopsis thaliana* leaf margin development. Proc Natl Acad Sci USA **108:** 3424–3429

Brand U, Fletcher JC, Hobe M, Meyerowitz EM, Simon R (2000) Dependence of stem cell fate in Arabidopsis on a feedback loop regulated by CLV3 activity. Science **289:** 617–619

Brewer PB, Howles PA, Dorian K, Griffith ME, Ishida T, Kaplan-Levy RN, Kilinc A, Smyth DR (2004) *PETAL LOSS*, a trihelix transcription factor gene, regulates perianth architecture in the Arabidopsis flower. Development **131:** 4035–4045

Cartolano M, Pieper B, Lempe J, Tattersall A, Huijser P, Tresch A, Darrah PR, Hay A, Tsiantis M (2015) Heterochrony underpins natural variation in *Cardamine hirsuta* leaf form. Proc Natl Acad Sci USA **112:** 10539–10544

Clark SE, Running MP, Meyerowitz EM (1993) *CLAVATA1*, a regulator of meristem and flower development in *Arabidopsis*. Development **119:** 397–418

Clark SE, Running MP, Meyerowitz EM (1995) *CLAVATA3* is a specific regulator of shoot and floral meristem development affecting the same processes as *CLAVATA1*. Development **121:** 2057–2067

Clark SE, Williams RW, Meyerowitz EM (1997) The *CLAVATA1* gene encodes a putative receptor kinase that controls shoot and floral meristem size in Arabidopsis. Cell **89:** 575–585

Coen ES, Meyerowitz EM (1991) The war of the whorls: Genetic interactions controlling flower development. Nature **353:** 31–37

Corbesier L, Vincent C, Jang S, Fornara F, Fan Q, Searle I, Giakountis A, Farrona S, Gissot L, Turnbull C, et al (2007) FT protein movement contributes to long-distance signaling in floral induction of Arabidopsis. Science **316:** 1030–1033

Eriksson S, Böhlenius H, Moritz T, Nilsson O (2006) GA4 is the active gibberellin in the regulation of LEAFY transcription and Arabidopsis floral initiation. Plant Cell **18:** 2172–2181

Fletcher JC (2001) The *ULTRAPETALA* gene controls shoot and floral meristem size in Arabidopsis. Development **128:** 1323–1333

Fletcher JC, Brand U, Running MP, Simon R, Meyerowitz EM (1999) Signaling of cell fate decisions by CLAVATA3 in Arabidopsis shoot meristems. Science **283:** 1911–1914

Gan X, Hay A, Kwantes M, Haberer G, Hallab A, Ioio RD, Hofhuis H, Pieper B, Cartolano M, Neumann U, et al (2016) The *Cardamine hirsuta* genome offers insight into the evolution of morphological diversity. Nat Plants **2:** 16167

Gan Y, Yu H, Peng J, Broun P (2007) Genetic and molecular regulation by DELLA proteins of trichome development in Arabidopsis. Plant Physiol **145:** 1031–1042

Griffith ME, da Silva Conceição A, Smyth DR (1999) *PETAL LOSS* gene regulates initiation and orientation of second whorl organs in the Arabidopsis flower. Development **126:** 5635–5644

Gu X, Le C, Wang Y, Li Z, Jiang D, Wang Y, He Y (2013) Arabidopsis FLC clade members form flowering-repressor complexes coordinating responses to endogenous and environmental cues. Nat Commun **4:** 1947

Guo AY, Zhu QH, Gu X, Ge S, Yang J, Luo J (2008) Genome-wide identification and evolutionary analysis of the plant specific SBP-box transcription factor family. Gene **418:** 1–8

Hartmann U, Höhmann S, Nettesheim K, Wisman E, Saedler H, Huijser P (2000) Molecular cloning of SVP: A negative regulator of the floral transition in Arabidopsis. Plant J **21:** 351–360

Hay AS, Pieper B, Cooke E, Mandáková T, Cartolano M, Tattersall AD, Ioio RD, McGowan SJ, Barkoulas M, Galinha C, et al (2014) *Cardamine hirsuta*: A versatile genetic system for comparative studies. Plant J **78:** 1–15

Hay A, Tsiantis M (2006) The genetic basis for differences in leaf form between *Arabidopsis thaliana* and its wild relative *Cardamine hirsuta*. Nat Genet **38:** 942–947

Hofhuis H, Moulton D, Lessinnes T, Routier-Kierzkowska AL, Bomphrey RJ, Mosca G, Reinhardt H, Sarchet P, Gan X, Tsiantis M, et al (2016) Morphomechanical innovation drives explosive seed dispersal. Cell **166:** 222–233

Honma T, Goto K (2001) Complexes of MADS-box proteins are sufficient to convert leaves into floral organs. Nature **409:** 525–529

Huang T, Irish VF (2016) Gene networks controlling petal organogenesis. J Exp Bot **67:** 61–68

Huang T, López-Giráldez F, Townsend JP, Irish VF (2012) RBE controls microRNA164 expression to effect floral organogenesis. Development **139:** 2161–2169

Huijser P, Schmid M (2011) The control of developmental phase transitions in plants. Development **138:** 4117–4129

Hyun Y, Richter R, Vincent C, Martinez-Gallegos R, Porri A, Coupland G (2016) Multi-layered regulation of SPL15 and cooperation with SOC1 integrate endogenous flowering pathways at the Arabidopsis shoot meristem. Dev Cell **37:** 254–266

Irish VF (2008) The Arabidopsis petal: A model for plant organogenesis. Trends Plant Sci **13:** 430–436

Jung JH, Domijan M, Klose C, Biswas S, Ezer D, Gao M, Khattak AK, Box MS, Charoensawan V, Cortijo S, et al (2016) Phytochromes function as thermosensors in Arabidopsis. Science **354:** 886–889

Kardailsky I, Shukla VK, Ahn JH, Dagenais N, Christensen SK, Nguyen JT, Chory J, Harrison MJ, Weigel D (1999) Activation tagging of the floral inducer FT. Science **286:** 1962–1965

Kaufmann K, Muiño JM, Jauregui R, Airoldi CA, Smaczniak C, Krajewski P, Angenent GC (2009) Target genes of the MADS transcription factor SEPALLATA3: integration of developmental and hormonal pathways in the Arabidopsis flower. PLoS Biol **7:** e1000090

Kayes JM, Clark SE (1998) CLAVATA2, a regulator of meristem and organ development in Arabidopsis. Development **125:** 3843–3851

Kobayashi Y, Kaya H, Goto K, Iwabuchi M, Araki T (1999) A pair of related genes with antagonistic roles in mediating flowering signals. Science **286:** 1960–1962

Koornneef M, Blankestijndevries H, Hanhart C, Soppe W, Peeters T (1994) The phenotype of some late-flowering mutants is enhanced by a locus on chromosome-5 that is not effective in the Landsberg *erecta* wild-type. Plant J **6:** 911–919

Krizek BA, Fletcher JC (2005) Molecular mechanisms of flower development: An armchair guide. Nat Rev Genet **6:** 688–698

Kumar SV, Wigge PA (2010) H2A.Z-containing nucleosomes mediate the thermosensory response in Arabidopsis. Cell **140:** 136–147

Lampugnani ER, Kilinc A, Smyth DR (2012) *PETAL LOSS* is a boundary gene that inhibits growth between developing sepals in *Arabidopsis thaliana*. Plant J **71:** 724–735

Lampugnani ER, Kilinc A, Smyth DR (2013) Auxin controls petal initiation in Arabidopsis. Development **140:** 185–194

Laufs P, Peaucelle A, Morin H, Traas J (2004) MicroRNA regulation of the CUC genes is required for boundary size control in Arabidopsis meristems. Development **131:** 4311–4322

Laux T, Mayer KFX, Berger J, Jürgens G (1996) The *WUSCHEL* gene is required for shoot and floral meristem integrity in Arabidopsis. Development **122:** 87–96

Lee I, Michaels SD, Masshardt AS, Amasino RM (1994) The late-flowering phenotype of *FRIGIDA* and mutations in *LUMINIDEPENDENS* is suppressed in the Landsberg *erecta* strain of *Arabidopsis*. Plant J **6:** 903–909

Lee JH, Ryu HS, Chung KS, Posé D, Kim S, Schmid M, Ahn JH (2013) Regulation of temperature-responsive flowering by MADS-box transcription factor repressors. Science **342:** 628–632

Lee JH, Yoo SJ, Park SH, Hwang I, Lee JS, Ahn JH (2007) Role of SVP in the control of flowering time by ambient temperature in Arabidopsis. Genes Dev **21:** 397–402

Legris M, Klose C, Burgie ES, Rojas CC, Neme M, Hiltbrunner A, Wigge PA, Schäfer E, Vierstra RD, Casal JJ (2016) Phytochrome B integrates light and temperature signals in Arabidopsis. Science **354:** 897–900

Lenhard M, Bohnert A, Jürgens G, Laux T (2001) Termination of stem cell maintenance in Arabidopsis floral meristems by interactions between WUSCHEL and AGAMOUS. Cell **105:** 805–814

Li D, Liu C, Shen L, Wu Y, Chen H, Robertson M, Helliwell CA, Ito T, Meyerowitz E, Yu H (2008) A repressor complex governs the integration of flowering signals in Arabidopsis. Dev Cell **15:** 110–120

Liu C, Xi W, Shen L, Tan C, Yu H (2009) Regulation of floral patterning by flowering time genes. Dev Cell **16:** 711–722

Liu C, Zhou J, Bracha-Drori K, Yalovsky S, Ito T, Yu H (2007) Specification of Arabidopsis floral meristem identity by repression of flowering time genes. Development **134:** 1901–1910

Lohmann JU, Hong RL, Hobe M, Busch MA, Parcy F, Simon R, Weigel D (2001) A molecular link between stem cell regulation and floral patterning in Arabidopsis. Cell **105:** 793–803

Mallory AC, Dugas DV, Bartel DP, Bartel B (2004) MicroRNA regulation of NAC-domain targets is required for proper formation and separation of adjacent embryonic, vegetative, and floral organs. Curr Biol **14:** 1035–1046

Mathieu J, Yant LJ, Mürdter F, Küttner F, Schmid M (2009) Repression of flowering by the miR172 target SMZ. PLoS Biol **7:** e1000148

Michaels SD, Amasino RM (1999) FLOWERING LOCUS C encodes a novel MADS domain protein that acts as a repressor of flowering. Plant Cell **11:** 949–956

Monniaux M, Pieper B, Hay A (2016) Stochastic variation in *Cardamine hirsuta* petal number. Ann Bot (Lond) **117:** 881–887

Muller AJ (1961) Zur Charakterisierung der Blüten und Infloreszenzen von *Arabidopsis thaliana* (L.) Heynh. Kulturpflanze **9:** 364–393

Parcy F, Nilsson O, Busch MA, Lee I, Weigel D (1998) A genetic framework for floral patterning. Nature **395:** 561–566

Park SJ, Eshed Y, Lippman ZB (2014) Meristem maturation and inflorescence architecture—lessons from the Solanaceae. Curr Opin Plant Biol **17:** 70–77

Park SJ, Jiang K, Schatz MC, Lippman ZB (2012) Rate of meristem maturation determines inflorescence architecture in tomato. Proc Natl Acad Sci USA **109:** 639–644

Pelaz S, Ditta GS, Baumann E, Wisman E, Yanofsky MF (2000) B and C floral organ identity functions require SEPALLATA MADS-box genes. Nature **405:** 200–203

Pieper B, Monniaux M, Hay A (2016) The genetic architecture of petal number in *Cardamine hirsuta.* New Phytol **209:** 395–406

Posé D, Verhage L, Ott F, Yant L, Mathieu J, Angenent GC, Immink RG, Schmid M (2013) Temperature-dependent regulation of flowering by antagonistic FLM variants. Nature **503:** 414–417

Ratcliffe OJ, Kumimoto RW, Wong BJ, Riechmann JL (2003) Analysis of the Arabidopsis MADS AFFECTING FLOWERING gene family: MAF2 prevents vernalization by short periods of cold. Plant Cell **15:** 1159–1169

Running MP, Fletcher JC, Meyerowitz EM (1998) The *WIGGUM* gene is required for proper regulation of floral meristem size in Arabidopsis. Development **125:** 2545–2553

Samach A, Onouchi H, Gold SE, Ditta GS, Schwarz-Sommer Z, Yanofsky MF, Coupland G (2000) Distinct roles of CONSTANS target genes in reproductive development of Arabidopsis. Science **288:** 1613–1616

Schoof H, Lenhard M, Haecker A, Mayer KF, Jürgens G, Laux T (2000) The stem cell population of Arabidopsis shoot meristems in maintained by a regulatory loop between the *CLAVATA* and *WUSCHEL* genes. Cell **100:** 635–644

Shikata M, Koyama T, Mitsuda N, Ohme-Takagi M (2009) Arabidopsis SBP-box genes *SPL10, SPL11* and *SPL2* control morphological change in association with shoot maturation in the reproductive phase. Plant Cell Physiol **50:** 2133–2145

Sicard A, Lenhard M (2011) The selfing syndrome: a model for studying the genetic and evolutionary basis of morphological adaptation in plants. Ann Bot (Lond) **107:** 1433–1443

Smith RS, Guyomarc'h S, Mandel T, Reinhardt D, Kuhlemeier C, Prusinkiewicz P (2006) A plausible model of phyllotaxis. Proc Natl Acad Sci USA **103:** 1301–1306

Smyth DR, Bowman JL, Meyerowitz EM (1990) Early flower development in Arabidopsis. Plant Cell **2:** 755–767

Specht CD, Bartlett ME (2009) Flower evolution: The origin and subsequent diversification of the angiosperm flower. Annu Rev Ecol Evol Syst **40:** 217–243

Sung S, Amasino RM (2004) Vernalization in *Arabidopsis thaliana* is mediated by the PHD finger protein VIN3. Nature **427:** 159–164

Sureshkumar S, Dent C, Seleznev A, Tasset C, Balasubramanian S (2016) Nonsense-mediated mRNA decay modulates FLM-dependent thermosensory flowering response in Arabidopsis. Nat Plants **2:** 16055

Talbert PB, Henikoff S (2014) Environmental responses mediated by histone variants. Trends Cell Biol **24:** 642–650

Torti S, Fornara F, Vincent C, Andrés F, Nordström K, Göbel U, Knoll D, Schoof H, Coupland G (2012) Analysis of the Arabidopsis shoot meristem transcriptome during floral transition identifies distinct regulatory patterns and a leucine-rich repeat protein that promotes flowering. Plant Cell **24:** 444–462

Wagner D (2009) Flower morphogenesis: Timing is key. Dev Cell **16:** 621–622

Wagner D, Sablowski RW, Meyerowitz EM (1999) Transcriptional activation of *APETALA1* by LEAFY. Science **285:** 582–584

Wang J-W, Czech B, Weigel D (2009) miR156-regulated SPL transcription factors define an endogenous flowering pathway in *Arabidopsis thaliana.* Cell **138:** 738–749

Wei S, Gruber MY, Yu B, Gao MJ, Khachatourians GG, Hegedus DD, Parkin IA, Hannoufa A (2012) Arabidopsis mutant *sk156* reveals complex regulation of SPL15 in a miR156-controlled gene network. BMC Plant Biol **12:** 169

Weigel D, Alvarez J, Smyth DR, Yanofsky MF, Meyerowitz EM (1992) LEAFY controls floral meristem identity in Arabidopsis. Cell **69:** 843–859

Wu G, Park MY, Conway SR, Wang J-W, Weigel D, Poethig RS (2009) The sequential action of miR156 and miR172 regulates developmental timing in Arabidopsis. Cell **138:** 750–759

Yamaguchi N, Winter CM, Wu MF, Kanno Y, Yamaguchi A, Seo M, Wagner D (2014) Gibberellin acts positively then negatively to control onset of flower formation in Arabidopsis. Science **344:** 638–641

Yu H, Ito T, Wellmer F, Meyerowitz EM (2004) Repression of AGAMOUS-LIKE 24 is a crucial step in promoting flower development. Nat Genet **36:** 157–161

Yu N, Cai WJ, Wang S, Shan CM, Wang LJ, Chen XY (2010) Temporal control of trichome distribution by microRNA156-targeted *SPL* genes in *Arabidopsis thaliana.* Plant Cell **22:** 2322–2335

Yu S, Galvão VC, Zhang YC, Horrer D, Zhang TQ, Hao YH, Feng YQ, Wang S, Schmid M, Wang JW (2012) Gibberellin regulates the Arabidopsis floral transition through miR156-targeted SQUAMOSA promoter binding-like transcription factors. Plant Cell **24:** 3320–3332